Electronic Supplementary Material (ESI) for ChemComm.

A novel, rationally designed lanthanoid chelating tag delivers large paramagnetic structural restraints for biomolecular NMR

Supporting Information

Daniel Joss,[a] Florine Winter,[a] and Daniel Häussinger*[a]

[a] Department of Chemistry, University of Basel, St. Johanns-Ring 19, CH-4056 Basel, daniel.haeussinger@unibas.ch

General Remarks

Unless otherwise stated, reactions were performed under an argon atmosphere and chemicals were used as received without further purification. All reactions were executed in anhydrous solvents, while technical grade solvents were used for extractions and flash column chromatography.

Silica gel 60 F_{254} on aluminium sheets from Merck was used for thin layer chromatography. The detection was either monitored with an UV-lamp at a wavelength of 254 nm or with potassium permanganate stain.

NMR experiments were performed at a temperature of 298 K on Bruker Avance III NMR spectrometers operating at 400, 500 and 600 MHz. ESI-MS spectra were recorded on a Shimadzu LCMS-2020 liquid chromatograph mass spectrometer. HRMS spectra were measured on a Bruker MaXis 4G HiRes ESI Mass Spectrometer.

Fitting of kinetic data and PRE analysis were performed using OriginPro 2018 (OriginLab, Northampton, MA, United States). Theoretical PRE were calculated using the reduced Solomon-Bloembergen equation with J=7/2 for Gd and rotational correlation times for both protein constructs approximated with 0.6 x molecular mass of the LCT-protein constructs (5.7 ns for ubiquitin S57C labelled with Gd-M7-Nitro and 18.1 ns for hCA S50C labelled with Gd-M7-Nitro).[1] I_{para}/I_{dia} ratios were normalized using the I_{para}/I_{dia} ratio of the most distant residue. Tri-*tert*-butyl 2,2',2''-((2*S*,5*S*,8*S*,11*S*)-2,5,8,11-tetramethyl-1,4,7,10-tetraazacyclododecane-1,4,7-triyl)-(2*R*,2'*R*,2''*R*)-tripropionate was synthesized according to the published procedures by Müntener et al.[2] Ubiquitin S57C was expressed as described previously by Sass et al.,[3] selectively ^{15}N leucine labelled hCA II S50C as described by Varghese et al.[4] Tagging reactions were performed in 10 mM phosphate and 0.2 mM TCEP buffer with pH 7.0 (ubiquitin S57C) or pH 6.8 (hCA S50C) at rt overnight. ^{1}H-^{15}N HSQC and ^{1}H-^{15}N HSQC IPAP spectra were measured in 10 mM phosphate buffer with pH 6.0 (ubiquitin S57C, ca. 100 µM) and pH 6.8 (hCA II S50C, ca. 200 µM) at a temperature of 298 K on a 600 MHz Bruker Avance III NMR spectrometer equipped with a cryogenic QCI-F probe. The obtained NMR spectra were assigned using CcpNmr Analysis.[5] The tensor properties were then obtained by fitting the residues in secondary structure elements of ubiquitin (PDB 1UBI)[6] or the leucine residues of hCA II (PDB 3KS3)[7] using Numbat (PCSs) with correction for residual anisotropic chemical shifts (RACS),[8] while RDCs were fitted using Fanten (with order parameter S^2 = 0.9) and Paramagpy.[9-10] Absolute deviation values of axial and rhombic components of PCS-derived tensors using Numbat were estimated by a Monte-Carlo simulation with a perturbation level of 0.1 Å on the protein structure and 10000 iterations. The metal centres were found in a distance of 6.9 Å (ubiquitin S57C) and 7.1 Å (hCA II S50C) from the C_{beta} of the cysteine residue. Q-factors were calculated using the following equation:

$$Q = \frac{\sqrt{\sum \left(PCS_{exp} - PCS_{calc}\right)^2}}{\sqrt{\sum \left(PCS_{exp}\right)^2}}.$$

HPLC conditions

Analytical HPLC measurements were performed on a Shimadzu LC system (LC-20AT prominence liquid chromatograph, SIL-20A HT prominence auto sampler, CTO-20AC prominence column oven, CBM-20A communications bus module, SPD-20A prominence UV/VIS detector (λ = 254 and 280 nm), LC-20AD prominence liquid chromatograph) combined with a Shimadzu LCMS-2020 liquid chromatograph mass spectrometer. As column for analytical HPLC measurements, a ReproSil-Pur ODS, 3.3 µm, 150 x 3 mm, provided by Maisch GmbH was used. Commercial HPLC grade solvents were used and a binary gradient was applied.

Solvent A: Milli-Q water + 0.1% TFA

Solvent B: 90% acetonitrile + 10% Milli-Q water + 0.085% TFA.

HPLC gradient: 95% A (min 0-2), linear gradient 95% A to 100% B (min 2-6), 100% B (min 6-14), linear gradient 100% B to 95% A (min 14-15), 95% A (min 15-22).

Semi-preparative HPLC purification was performed on a Shimadzu LC system (LC-20AT prominence liquid chromatograph, SIL-20A HT prominence auto sampler, CTO-20AC prominence column oven, CBM-20A communications bus module, SPD-20A prominence UV/VIS detector (λ = 254 and 280 nm), LC-20AD prominence liquid chromatograph) combined with a Shimadzu LCMS-2020 liquid chromatograph mass spectrometer. As column for preparative HPLC purification, a ReproSil-Pur 120 ODS-3, 5 µm, 150 x 20 mm, provided by Maisch GmbH was used. Commercial HPLC grade solvents were used and a binary gradient was applied during purification.

Solvent A: Milli-Q water + 0.1% TFA

Solvent B: 90% acetonitrile + 10% Milli-Q water + 0.085% TFA.

HPLC gradient: 95% A (min 0-2), linear gradient 95% A to 100% B (min 2-15), 100% B (min 15-22), linear gradient 100% B to 95% A (min 22-23), 95% A (min 23-25).

HPLC measurements of protein samples were performed using the direct injection mode on a Shimadzu LC system (LC-20AT prominence liquid chromatograph, SIL-20A HT prominence auto sampler, CTO-20AC prominence column oven, CBM-20A communications bus module, SPD-20A prominence UV/VIS detector (λ = 254 and 280 nm), LC-20AD prominence liquid chromatograph) combined with a Shimadzu LCMS-2020 liquid chromatograph mass spectrometer. Commercial HPLC grade solvents were used and a binary gradient was applied. MS spectra of proteins were deconvoluted using the Bruker Daltonics DataAnalysis software.

Solvent A: Milli-Q water + 0.1% TFA

Solvent B: 90% acetonitrile + 10% Milli-Q water + 0.085% TFA.

HPLC gradient: isocratic 95% A (min 0-4).

6-Methyl-2-(methylthio)-3-nitropyridine

Sodium methanethiolate (487 mg, 6.95 mmol, 1.2 eq.) was added to a solution of 2-chloro-6-methyl-3-nitropyridine (1.00 g, 5.79 mmol, 1.0 eq.) in DMF (20 mL) at 0 °C and the mixture was stirred for 2.5 h at rt. The reaction mixture was then concentrated under reduced pressure and the crude was purified by flash column chromatography (SiO_2, cyclohexane:EtOAc, 9:1) to obtain 6-(bromomethyl)-2-(methylthio)-3-nitropyridine (760 mg, 4.13 mmol, 71%) as yellow solid.

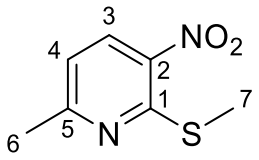

TLC (SiO_2, cyclohexane:EtOAc, 9:1): R_f = 0.27.

^{1}H-NMR (500 MHz, $CDCl_3$, δ/ppm): 8.38 (d, $^3J_{H3\text{-}H4}$ = 8.3 Hz, 1H, **H_3**), 7.00 (d, $^3J_{H4\text{-}H3}$ = 8.3 Hz, 1H, **H_4**), 2.63 (s, 3H, **H_6**), 2.57 (s, 3H, **H_7**).

^{13}C-NMR (126 MHz, $CDCl_3$, δ/ppm): 163.7 (**C_5**), 158.0 (**C_1**), 140.3 (**C_2**), 133.9 (**C_3**), 118.2 (**C_4**), 25.0 (**C_6**), 14.4 (**C_7**).

HRMS: $[M+H]^+$ $C_7H_9N_2O_2S$, m/z (calc.) = 185.0379, m/z (meas.) 185.0378.

6-(Bromomethyl)-2-(methylthio)-3-nitropyridine

N-Bromosuccinimide (930 mg, 5.23 mmol, 1.3 eq.) followed by dibenzoyl peroxide (130 mg, 0.402 mmol, 0.1 eq., 75%) was added to a solution of 6-methyl-2-(methylthio)-3-nitropyridine (741 mg, 4.02 mmol, 1.0 eq.) in dichloroethane (10 mL). The reaction mixture was heated to 80 °C and NBS (358 mg, 2.01 mmol, 0.5 eq.) and dibenzoyl peroxide (390 mg, 1.21 mmol, 0.3 eq., 75%) were added within 6 h. After 22 h, the reaction mixture was poured onto aq. sat. $NaHCO_3$ solution and the aq. layer was extracted with dichloromethane (3 x 10 ml). The combined organic layers were washed with brine, dried over anhydrous Na_2SO_4, filtered and concentrated *in vacuo*. The crude product was purified by flash column chromatography (SiO_2, cyclohexane:EtOAc, 19:1) to yield 6-(bromomethyl)-2-(methylthio)-3-nitropyridine (240 mg, 0.913 mmol, 23%) as a yellow solid.

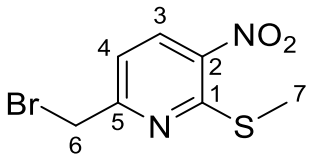

TLC (SiO_2, cyclohexane:EtOAc, 19:1): R_f = 0.16.

^{1}H-NMR (400 MHz, $CDCl_3$, δ/ppm): 8.49 (d, $^3J_{H3\text{-}H4}$ = 8.3 Hz, 1H, **H_3**), 7.30 (d, $^3J_{H4\text{-}H3}$ = 8.4 Hz, 1H, **H_4**), 4.55 (s, 2H, **H_6**), 2.59 (s, 3H, **H_7**).

^{13}C-NMR (126 MHz, $CDCl_3$, δ/ppm): 160.9 (**C_5**), 158.6 (**C_1**), 141.1 (**C_2**), 134.8 (**C_3**), 118.1 (**C_4**), 32.2 (**C_6**), 14.5 (**C_7**).

HRMS: $[M+H]^+$ $C_7H_8BrN_2O_2S$, m/z (calc.) = 262.9484, m/z (meas.) 262.9483.

Tri-*tert*-butyl 2,2',2''-((2*S*,5*S*,8*S*,11*S*)-2,5,8,11-tetramethyl-10-((6-(methylthio)-nitropyridin-2-yl)methyl)-1,4,7,10-tetraazacyclododecane-1,4,7-triyl)-(2*R*,2'*R*,2''*R*)-tripropionate

A solution of 6-(bromomethyl)-2-(methylthio)-3-nitropyridine (42.9 mg, 163 µmol, 2.0 eq.) in dry acetonitrile (1.0 mL) was added under argon to a suspension of tri-*tert*-butyl 2,2',2''-((2*S*,5*S*,8*S*,11*S*)-2,5,8,11-tetramethyl-1,4,7,10-tetraazacyclododecane-1,4,7-triyl)-(2*R*,2'*R*,2''*R*)-tripropionate (50.0 mg, 81.6 µmol, 1.0 eq.) and potassium carbonate (56.4 mg, 204 µmol, 5.0 eq.) in dry acetonitrile (1.0 mL). The reaction mixture was stirred for 24 h at rt. The suspension was filtered and the crude product was purified by prep. HPLC to obtain tri-*tert*-butyl 2,2',2''-((2*S*,5*S*,8*S*,11*S*)-2,5,8,11-tetramethyl-10-((6-(methylthio)-nitropyridin-2-yl)methyl)-1,4,7,10-tetraazacyclododecane-1,4,7-triyl)-(2*R*,2'*R*,2''*R*)-tripropionate (60.0 mg, 75.5 µmol, 93%) as a yellow oil.

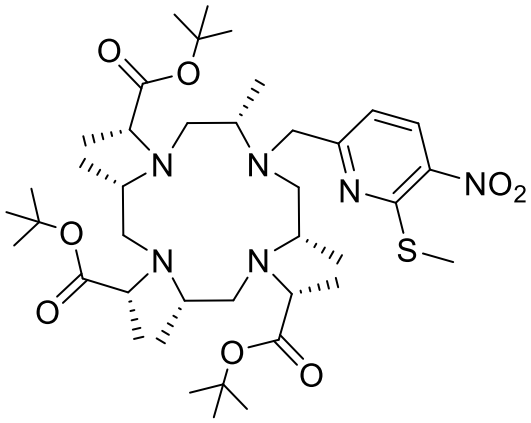

HRMS: $[M+H]^+$ $C_{40}H_{71}N_6O_8S$, m/z (calc.) = 795.5049, m/z (meas.) 795.5048.

(2*R*,2'*R*,2''*R*)-2,2',2''-((2*S*,5*S*,8*S*,11*S*)-2,5,8,11-tetramethyl-10-((6-(methylthio)-5-nitropyridin-2-yl)methyl)-1,4,7,10-tetraazacyclododecane-1,4,7-triyl) tripropionic acid

Tri-*tert*-butyl 2,2',2''-((2*S*,5*S*,8*S*,11*S*)-2,5,8,11-tetramethyl-10-((6-(methylthio)-5-nitropyridin-2-yl)methyl)-1,4,7,10-tetraazacyclododecane-1,4,7-triyl)-(2*R*,2'*R*,2''*R*)-tripropionate (60.0 mg, 75.5 µmol, 1.0 eq.) was dissolved in acetonitrile (1.0 mL) and aq. HCl (1 M, 2.0 mL). The resulting solution was heated to 80 °C for 6 h. Then the mixture was cooled to rt and purified by prep. HPLC to yield (2*R*,2'*R*,2''*R*)-2,2',2''-((2*S*,5*S*,8*S*,11*S*)-2,5,8,11-tetramethyl-10-((6-(methylthio)-5-nitropyridin-2-yl)methyl)-1,4,7,10-tetraazacyclododecane-1,4,7-triyl) tripropionic acid (34.5 mg, 55.0 µmol, 73%) as a white solid.

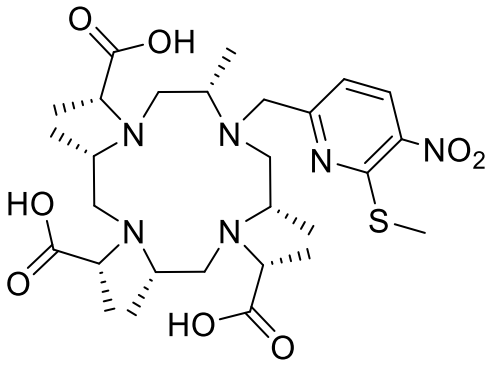

HRMS: $[M+H]^+$ $C_{28}H_{47}N_6O_8S$, m/z (calc.) = 627.3171, m/z (meas.) 627.3175.

Ln-(2*R*,2'*R*,2''*R*)-2,2',2''-((2*S*,5*S*,8*S*,11*S*)-2,5,8,11-tetramethyl-10-((6-(methylthio)-5-nitropyridin-2-yl)methyl)-1,4,7,10-tetraazacyclododecane-1,4,7-triyl) tripropanoate, Ln-M7-Nitro-SMe

LnX_3 (4.0 eq.) was added to a solution of (2*R*,2'*R*,2''*R*)-2,2',2''-((2*S*,5*S*,8*S*,11*S*)-2,5,8,11-tetramethyl-10-((6-(methylthio)-5-nitropyridin-2-yl)methyl)-1,4,7,10-tetraazacyclododecane-1,4,7-triyl)-(2*R*,2'*R*,2''*R*)-tripropionic acid (1.0 eq.) in aq. ammonium acetate (100 mM). The reaction mixture was stirred in a pre-heated oil-bath at 80 °C. The reaction mixture was cooled to rt and purified by prep. HPLC to obtain the title compound **50a-e** as an off-white solid.

Table S1: Reaction conditions for the synthesis of Ln-M7-Nitro-SMe.

	Free Ligand	**aq. CH_3COONH_4**	**LnX_3**	**Time**	**Yield**
Lu	12.5 mg, 19.9 µmol	6 mL	$Lu(OTf)_3$ (49.8 mg, 80.0 µmol)	16 h	11.5 mg, 14.4 µmol, 72%
Tm	10.0 mg, 16.0 µmol	10 mL	$Tm(OTf)_3$ (19.7 mg, 31.9 µmol)	3.5 h	8.2 mg, 10.4 µmol, 65%
Dy	8.0 mg, 12.8 µmol	8 mL	$Dy(OTf)_3$ (31.2 mg, 51.2 µmol)	31 h	6.9 mg, 8.8 µmol, 69%
Tb	8.0 mg, 12.8 µmol	8 mL	$TbCl_3 \cdot 6\ H_2O$ (19.1 mg, 51.2 µmol	31 h	6.7 mg, 8.6 µmol, 67%
Gd	8.0 mg, 12.8 µmol	8 mL	$Gd(OTf)_3$ (30.9 mg, 51.2 µmol)	22 h	5.0 mg, 6.4 µmol, 50%
Yb	21.0 mg, 33.5 µmol	10 mL	$Yb(NO_3)_3 \cdot 5\ H_2O$ (60.4 mg, 134.0 µmol)	16 h	19.5 mg, 24.5 µmol, 73%

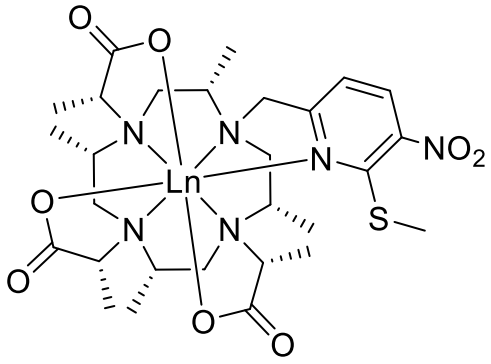

Lu: **HRMS**: $[M+H]^+$ $C_{28}H_{44}LuN_6O_8S$, m/z (calc.) = 799.2344, m/z (meas.) = 799.2343.

Tm: **HRMS**: $[M+H]^+$ $C_{28}H_{44}N_6O_8STm$, m/z (calc.) = 793.2278, m/z (meas.) = 793.2270.

Dy: **HRMS**: $[M+H]^+$ $C_{28}H_{44}DyN_6O_8S$, m/z (calc.) = 788.2228, m/z (meas.) = 788.2225.

Tb: **HRMS**: $[M+H]^+$ $C_{28}H_{44}N_6O_8STb$, m/z (calc.) = 783.2189, m/z (meas.) = 783.2185.

Gd: **HRMS**: $[M+H]^+$ $C_{28}H_{44}GdN_6O_8S$, m/z (calc.) = 782.2181, m/z (meas.) = 782.2179.

Yb: **HRMS**: $[M+Na]^+$ $C_{28}H_{43}NaN_6O_8SYb$, m/z (calc.) = 820.2148, m/z (meas.) = 820.2145.

Ln-(2*R*,2'*R*,2''*R*)-2,2',2''-((2*S*,5*S*,8*S*,11*S*)-2,5,8,11-tetramethyl-10-((6-(methylsulphonyl)-5-nitropyridin-2-yl)methyl)-1,4,7,10-tetraazacyclododecane-1,4,7-triyl) tripropanoate, Ln-M7-Nitro

Meta-chloroperoxybenzoic acid (77%) was added to a solution of Lu-(2*R*,2'*R*,2''*R*)-2,2',2''-((2*S*,5*S*,8*S*,11*S*)-2,5,8,11-tetramethyl-10-((6-(methylthio)-5-nitropyridin-2-yl)methyl)-1,4,7,10-tetraazacyclododecane-1,4,7-triyl)-(2*R*,2'*R*,2''*R*)-tripropanoate (1.0 eq.) in dichloromethane (1.0 - 5.0 mL). The resulting reaction mixture was stirred at rt. The reaction mixture was diluted with acetonitrile and dichloromethane was removed under reduced pressure. The remaining solution was purified by prep. HPLC to yield Ln-(2*R*,2'*R*,2''*R*)-2,2',2''-((2*S*,5*S*,8*S*,11*S*)-2,5,8,11-tetramethyl-10-((6-(methylsulphonyl)-5-nitropyridin-2-yl)methyl)-1,4,7,10-tetraazacyclododecane-1,4,7-triyl) tripropanoate as an off-white solid.

Table S2: Reaction conditions for the synthesis of Ln-M7-Nitro.

	Starting material	***m*-CPBA**	**Time**	**Yield**
Lu	6.5 mg, 8.1 µmol	9.1 mg, 40.7 µmol	19 h	4.0 mg, 4.8 µmol, 59%
Tm	4.0 mg, 5.1 µmol	5.7 mg, 25.3 µmol	22 h	2.0 mg, 2.4 µmol, 48%
Dy	14.0 mg, 17.8 µmol	39.9 mg, 178 µmol	16 h	4.5 mg, 2.4 µmol, 31%
Tb	13.0 mg, 16.6 µmol	37.2 mg, 166 µmol	16 h	5.0 mg, 6.1 µmol, 37%
Gd	5.0 mg, 6.4 µmol	7.2 mg, 32.0 µmol	42 h	1.5 mg, 1.9 µmol, 29%
Yb	19.5 mg, 24.5 µmol	110.0 mg, 490 µmol	16 h	10.0 mg, 12.1 µmol, 49%

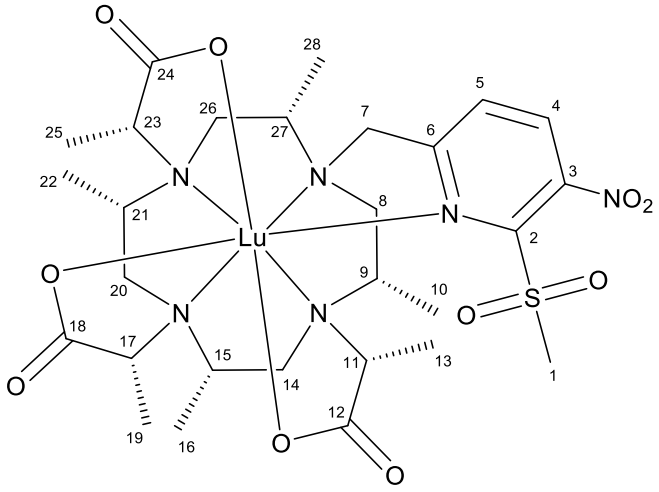

NMR-Assignment for Lu-M7-Nitro:

^{1}H-NMR (600 MHz, D_2O, δ/ppm): 8.56 (bs, 1H, **H_4**), 8.06 (d, $^{3}J_{H5\text{-}H4}$ = 8.3 Hz, 1H, **H_5**), 4.48 (d, ^{2}J = 14.4 Hz, 1H, **H_{7a}**), 4.43 (d, ^{2}J = 14.1 Hz, 1H, **H_{7b}**), 4.10 – 3.90 (m, 2H, **H_{11}**, **H_9**), 3.76 (q, $^{3}J_{H17\text{-}H19}$ = 7.3 Hz, 1H, **H_{17}**), 3.71 (q, $^{3}J_{H23\text{-}H25}$ = 7.2 Hz, 1H, **H_{23}**), 3.60 (s, 3H, **H_1**), 3.24 – 3.14 (m, 2H, **H_{27}**, **H_{8eq}**), 3.06 – 3.03 (m, 2H, **H_{14ax}**, **H_{15}**), 3.03 – 2.98 (m, 2H, **H_{26ax}**, **H_{21}**), 2.98 – 2.92 (m, 1H, **H_{20ax}**), 2.79 (d, $^{2}J_{H8ax\text{-}H8eq}$ = 15.3 Hz, 1H, **H_{8ax}**), 2.74 (d, $^{2}J_{H14eq\text{-}H14ax}$ = 12.2 Hz, 1H, **H_{14eq}**), 2.69 – 2.64 (m, 2H, **H_{26eq}**, **H_{20eq}**), 1.52 (d, $^{3}J_{H13\text{-}H11}$ = 7.1 Hz, 3H, **H_{13}**), 1.44 (d, $^{3}J_{H19\text{-}H17}$ = 7.4 Hz, 3H, **H_{19}**), 1.42 (d, $^{3}J_{H23\text{-}H25}$ = 7.0 Hz, 3H, **H_{25}**), 1.30 (d, $^{3}J_{H10\text{-}H9}$ = 6.5 Hz, 3H, **H_{10}**), 1.17 (d, $^{3}J_{H16\text{-}H15}$ = 5.6 Hz, 3H, **H_{16}**), 1.16 (d, $^{3}J_{H22\text{-}H21}$ = 6.2 Hz, 3H, **H_{22}**), 0.54 (bs, 3H, **H_{28}**).

^{13}C-NMR (151 MHz, D_2O, δ/ppm, extracted from HSQC and HMBC): 183.4 (**C_{18}**), 183.1 (**C_{24}**), 182.1 (**C_{12}**), 159.0 (**C_6**), 144.3 (**C_3**), 140.4 (**C_2**), 135.7 (**C_4**), 131.9 (**C_5**), 67.4 (**C_{17}**), 66.4 (**C_{11}**), 66.3 (**C_{23}**), 60.5 (**C_{21}**), 60.3 (**C_{15}**), 58.8 (**C_9**), 57.0 (**C_7**), 55.1 (**C_{27}**), 48.8 (**C_8**), 46.3 (**C_{27}**), 45.5 (**C_{14}**), 45.0 (**C_{26}**), 41.2 (**C_1**), 13.2 (**C_{19}**), 13.2 (**C_{16}**), 13.1 (**C_{13}**), 13.0 (**C_{25}**), 12.9 (**C_{10}**), 12.8 (**C_{22}**), 12.8 (**C_{28}**).

Lu: **HRMS**: $[M+H]^+$ $C_{28}H_{44}LuN_6O_{10}S$, m/z (calc.) = 831.2242, m/z (meas.) = 831.2231.

Tm: **HRMS**: $[M+H]^+$ $C_{28}H_{44}N_6O_{10}STm$, m/z (calc.) = 825.2176, m/z (meas.) = 825.2187.

Dy: **HRMS**: $[M+H]^+$ $C_{28}H_{44}DyN_6O_{10}S$, m/z (calc.) = 820.2126, m/z (meas.) = 820.2118.

Tb: **HRMS**: $[M+H]^+$ $C_{28}H_{44}N_6O_{10}STb$, m/z (calc.) = 815.2088, m/z (meas.) = 815.2079.

Gd: **HRMS**: $[M+H]^+$ $C_{28}H_{44}GdN_6O_{10}S$, m/z (calc.) = 814.2080, m/z (meas.) = 814.2076.

Yb: **HRMS**: $[M+H]^+$ $C_{28}H_{44}N_6O_{10}SYb$, m/z (calc.) = 830.2227, m/z (meas.) = 830.2224.

NMR spectra of synthesized compounds

^{1}H- and ^{13}C-NMR of 6-Methyl-2-(methylthio)-3-nitropyridine

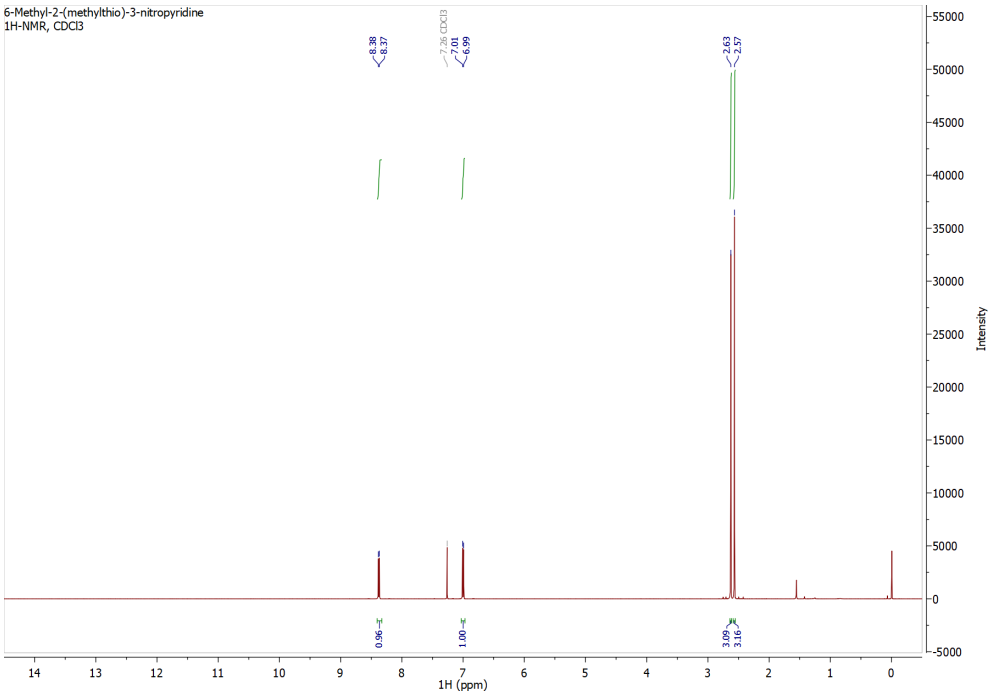

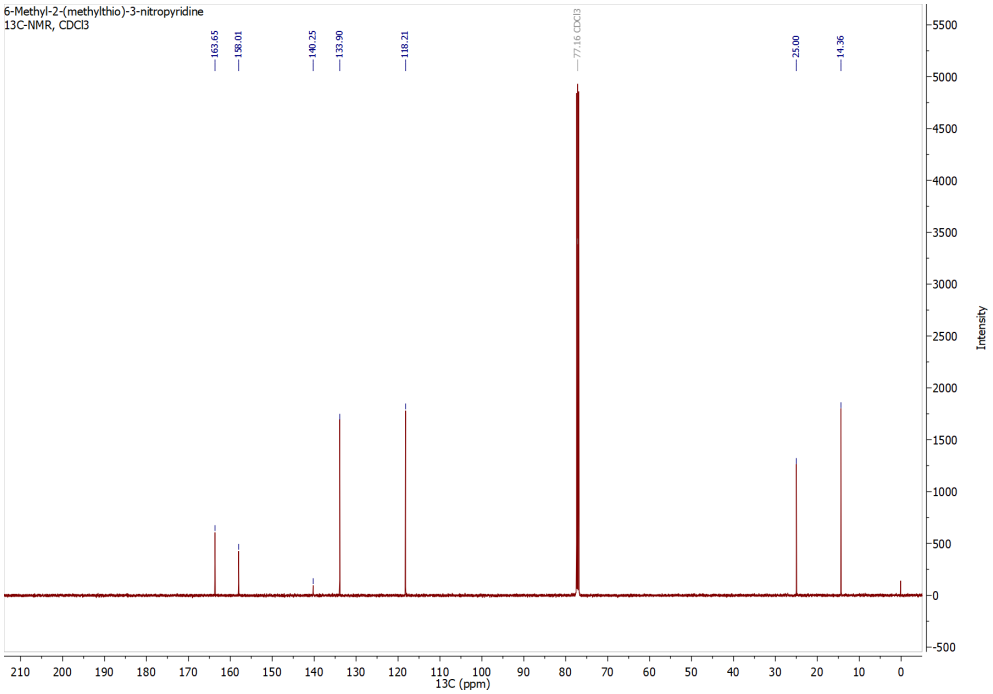

^{1}H- and ^{13}C-NMR of 6-(Bromomethyl)-2-(methylthio)-3-nitropyridine

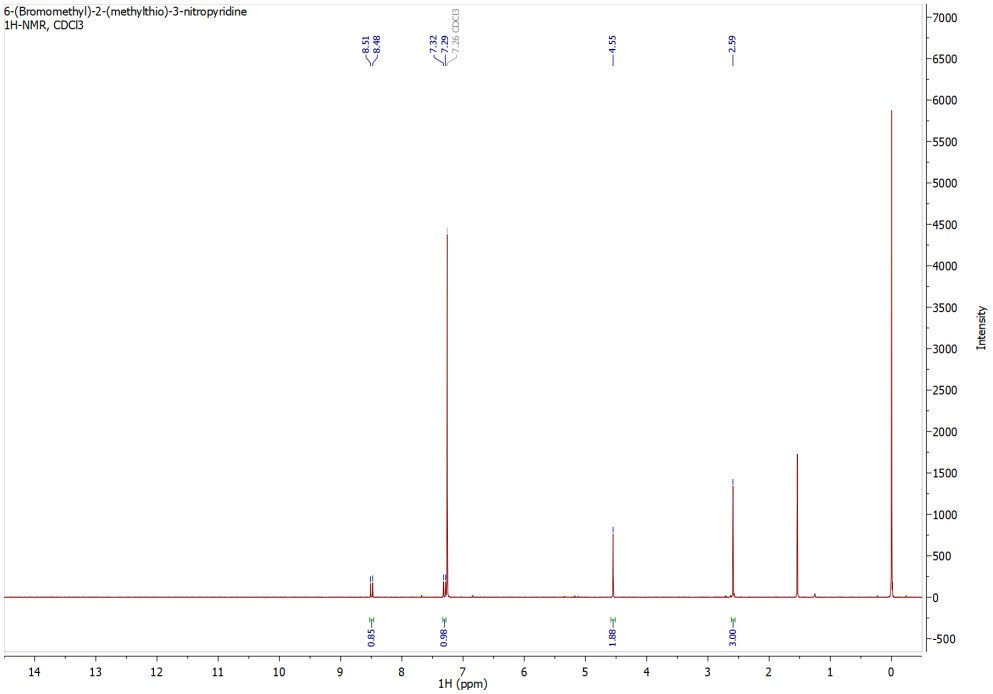

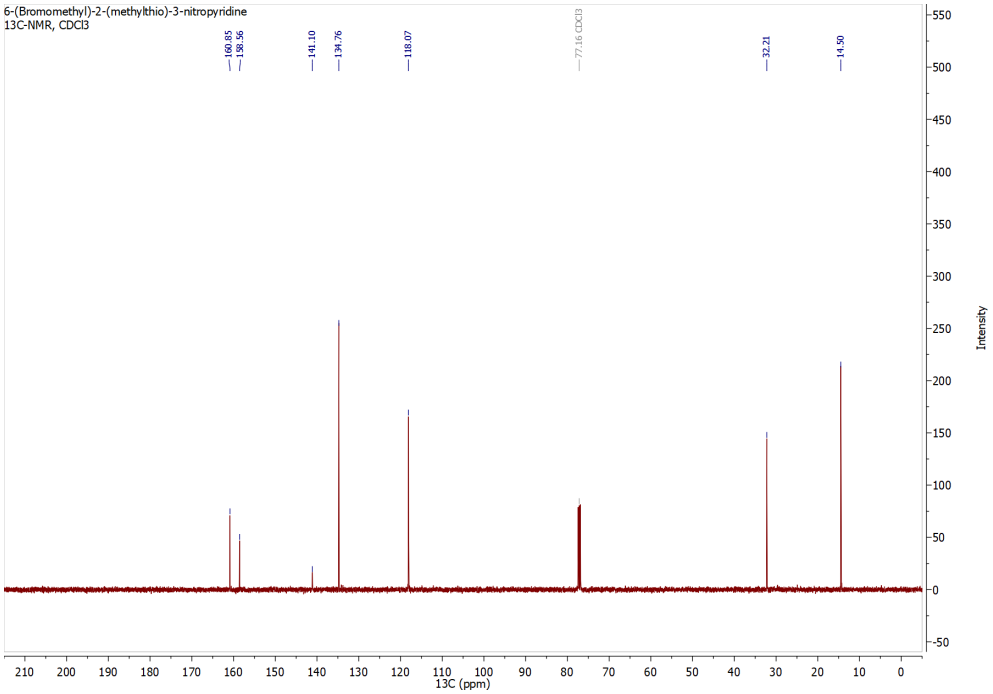

^{1}H NMR of Lu-M7-Nitro

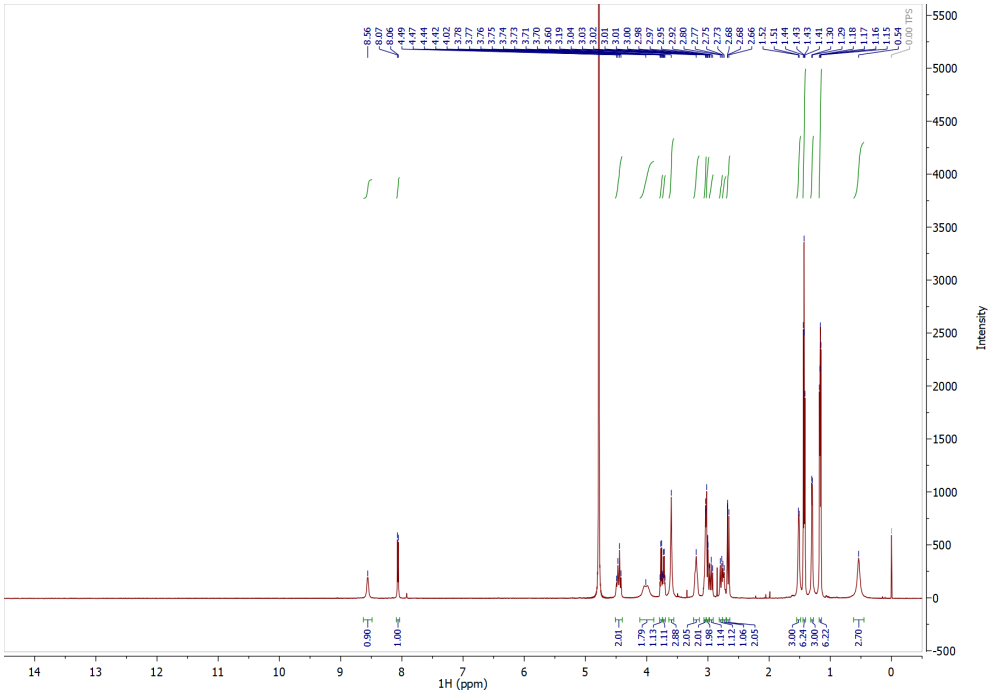

^{1}H-NMR of Tm-M7-Nitro

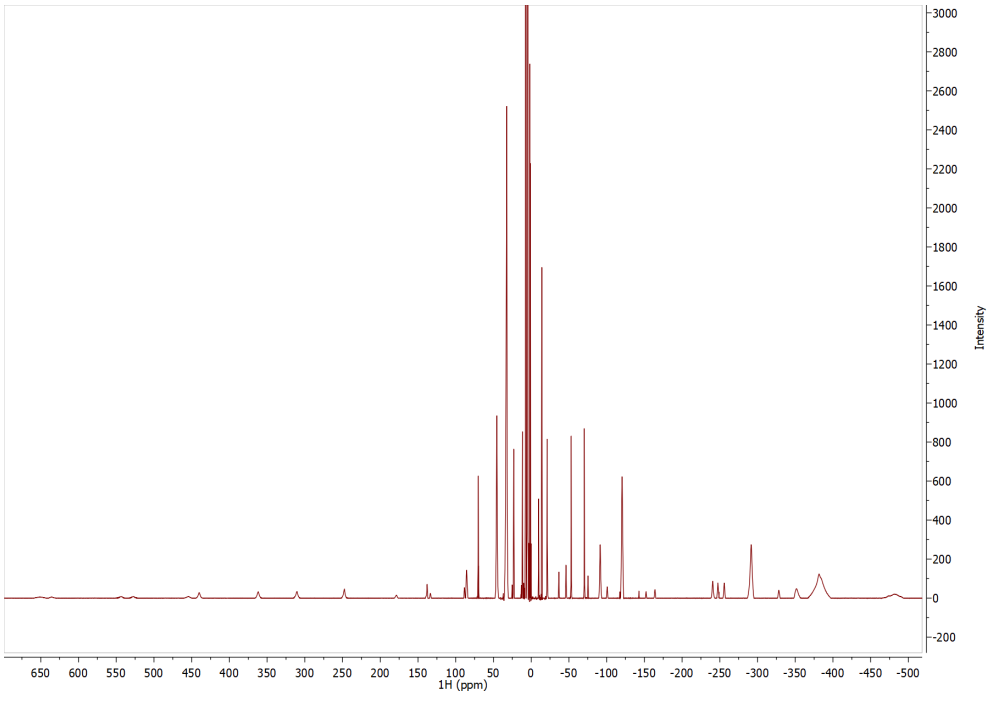

^{1}H-NMR of Dy-M7-Nitro

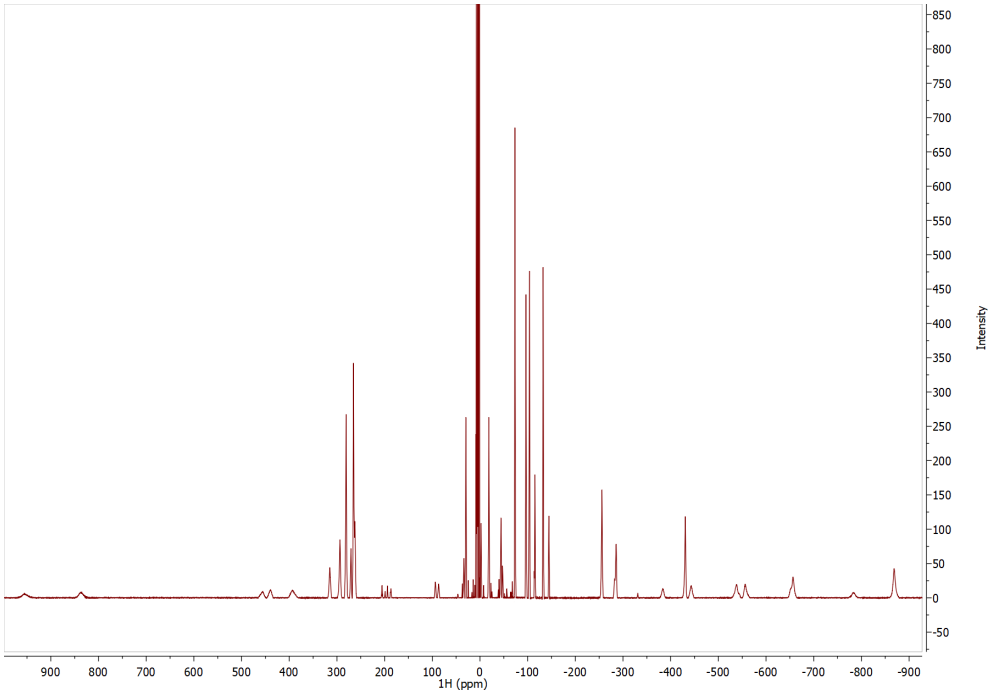

^{1}H-NMR of Tb-M7-Nitro

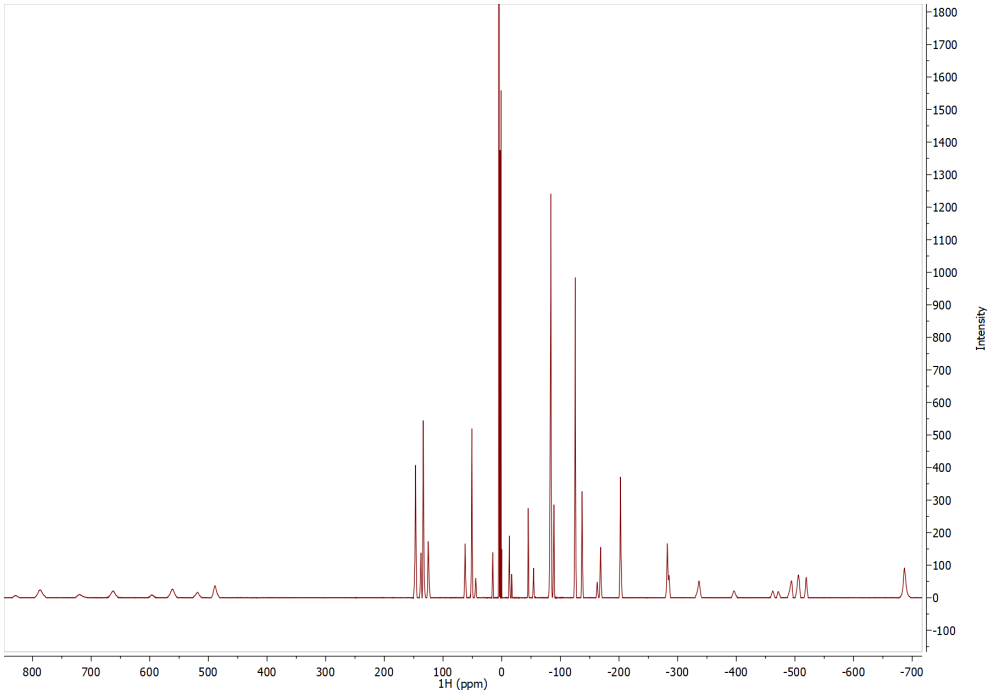

^{1}H-NMR of Yb-M7-Nitro

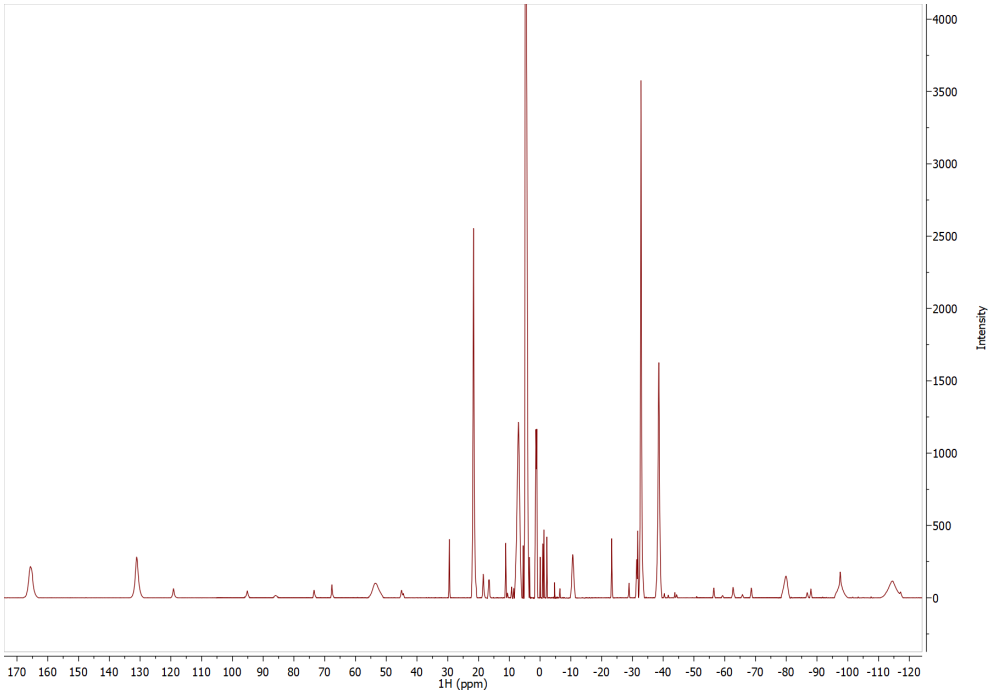

Analytical HPLC-ESI-MS measurement

Lu-M7-Nitro

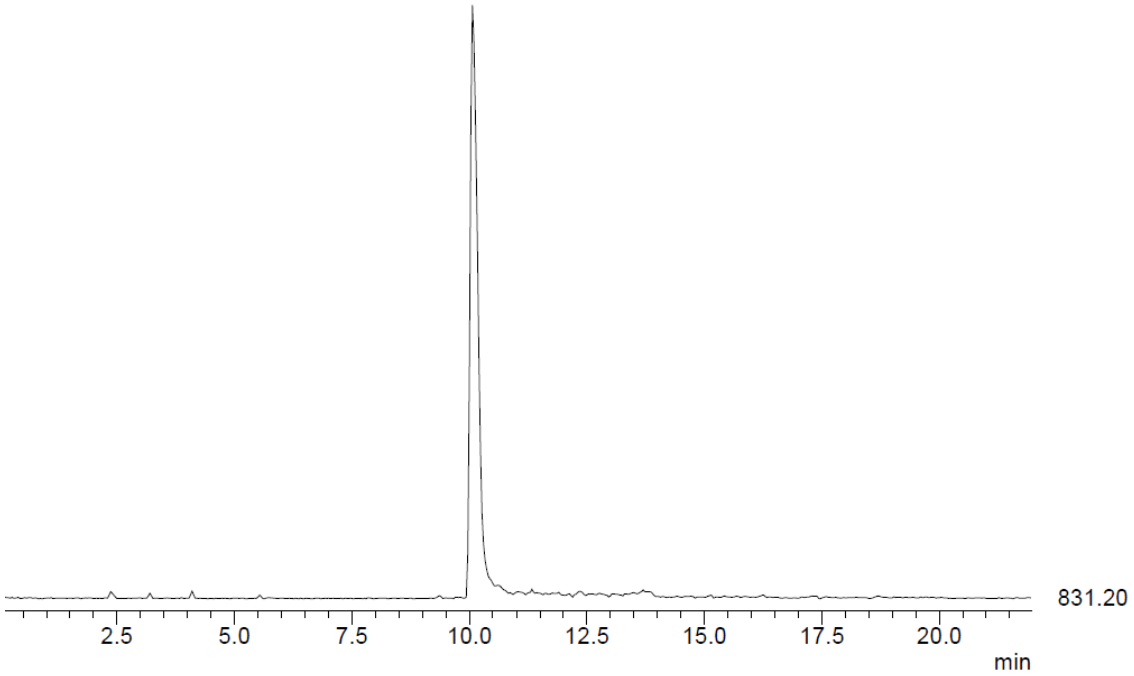

Figure S1: HPLC-ESI-MS trace of Lu-M7-Nitro.

Tm-M7-Nitro

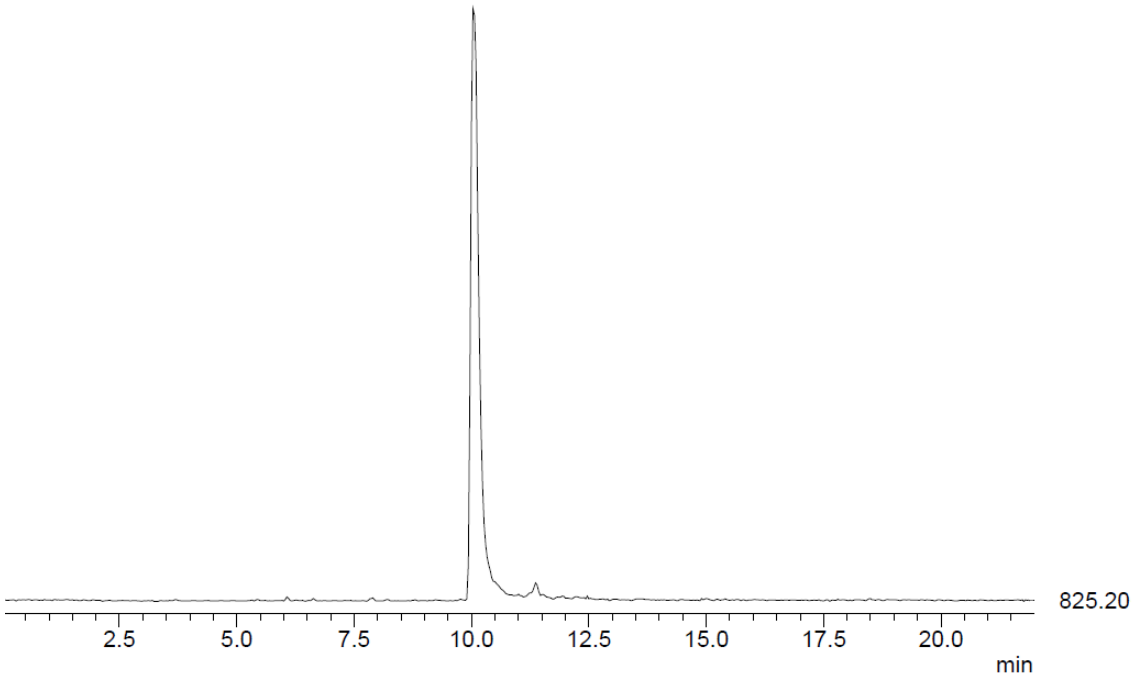

Figure S2: HPLC-ESI-MS trace of Tm-M7-Nitro.

Dy-M7-Nitro

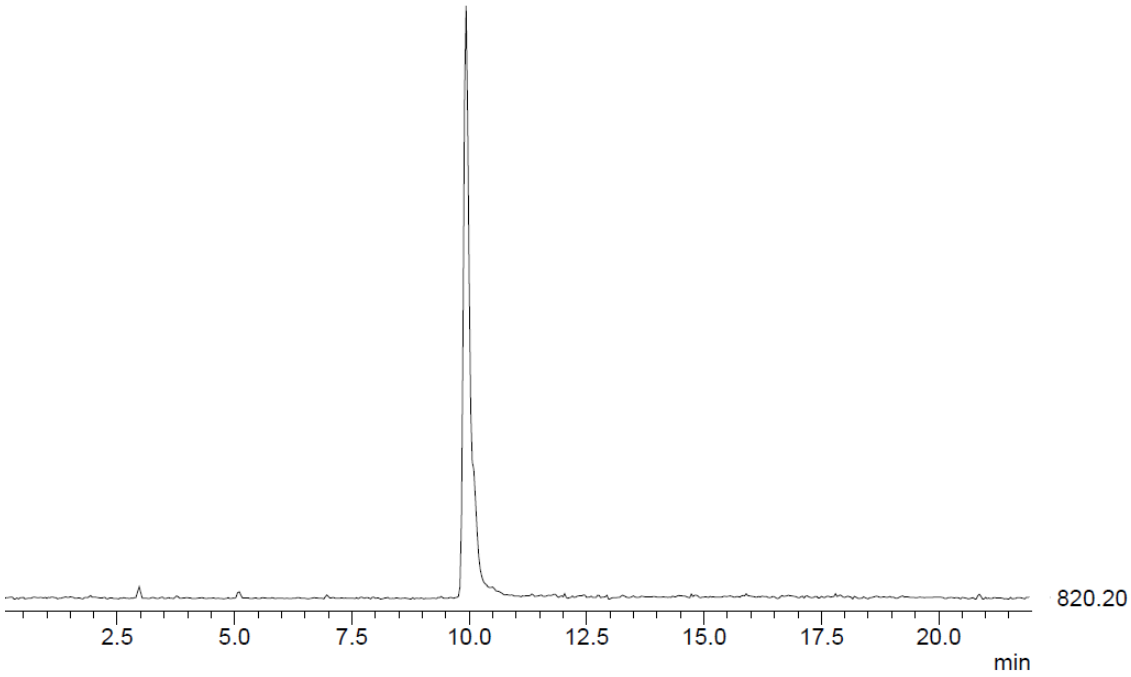

Figure S3: HPLC-ESI-MS trace of Dy-M7-Nitro.

Tb-M7-Nitro

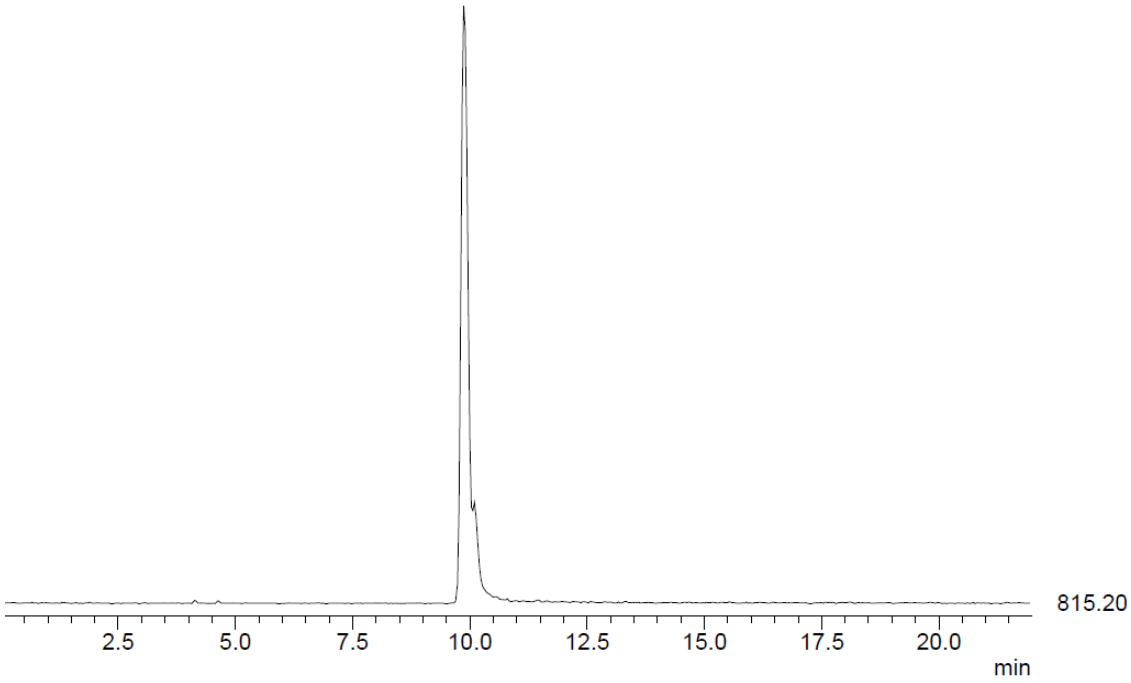

Figure S4: HPLC-ESI-MS trace of Tb-M7-Nitro.

Yb-M7-Nitro

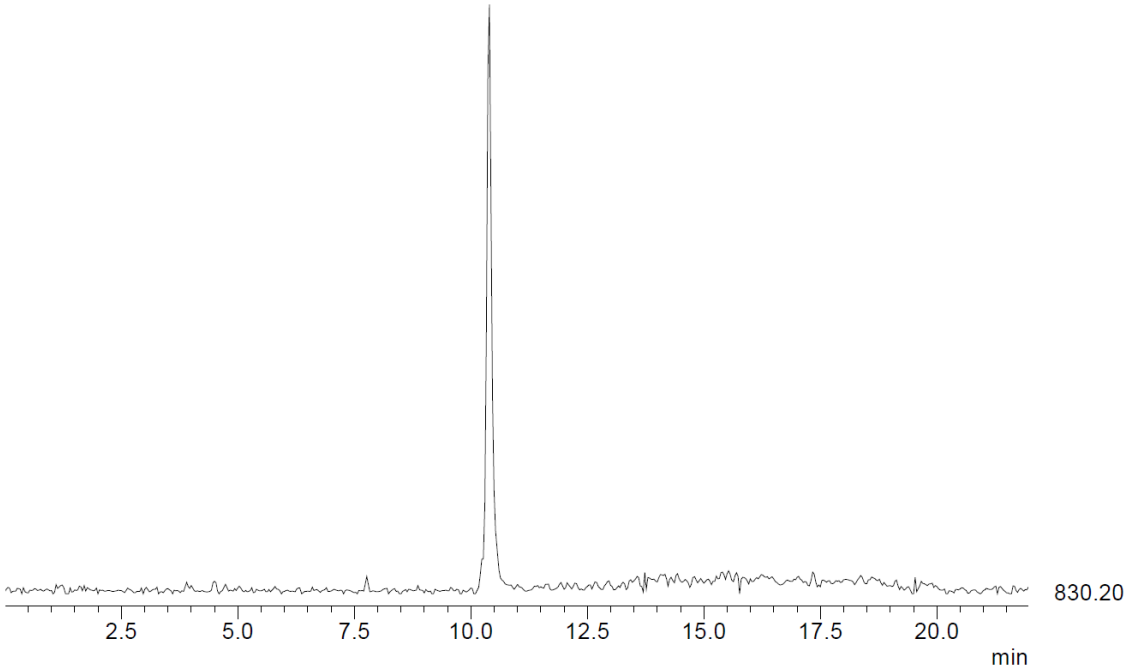

Figure S5: HPLC-ESI-MS trace of Yb-M7-Nitro.

Gd-M7-Nitro

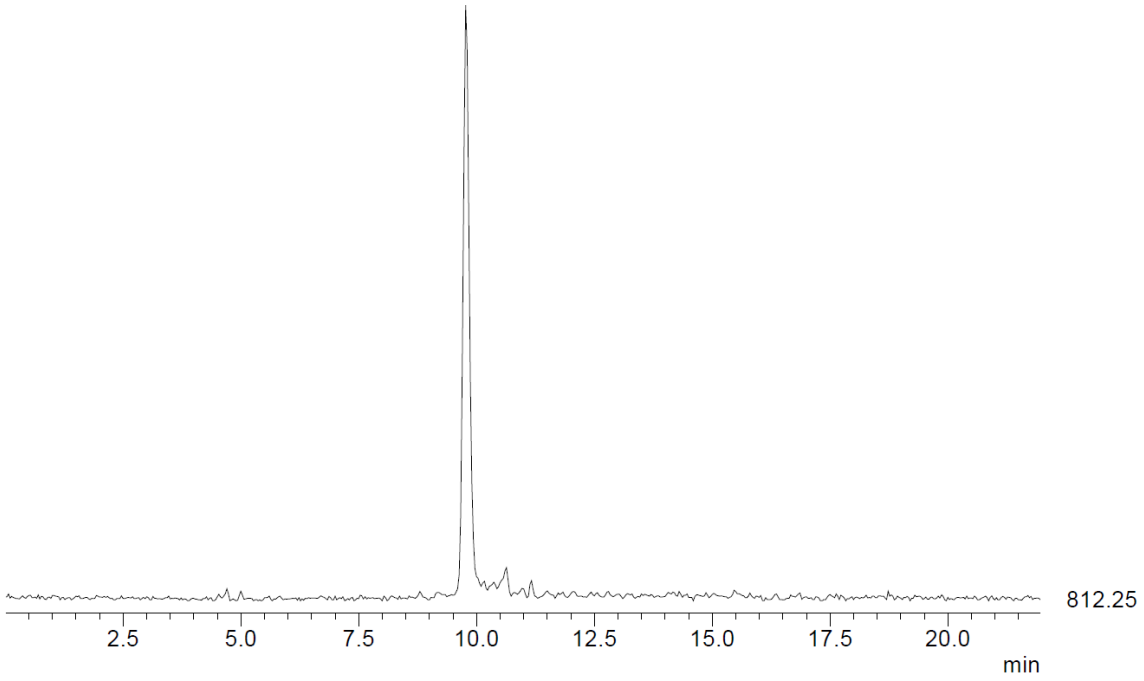

Figure S6: HPLC-ESI-MS trace of Gd-M7-Nitro.

Overlay of ^{1}H-^{15}N HSQC spectra of Tm- (red), Dy- (blue), Tb- (orange) and Lu-M7-Nitro-Ub^{S57C} (black)

Measured in 10 mM phosphate buffer with pH 6.0 at a temperature of 298 K on a 600 MHz Bruker Avance III NMR spectrometer equipped with a cryogenic QCI-F probe.

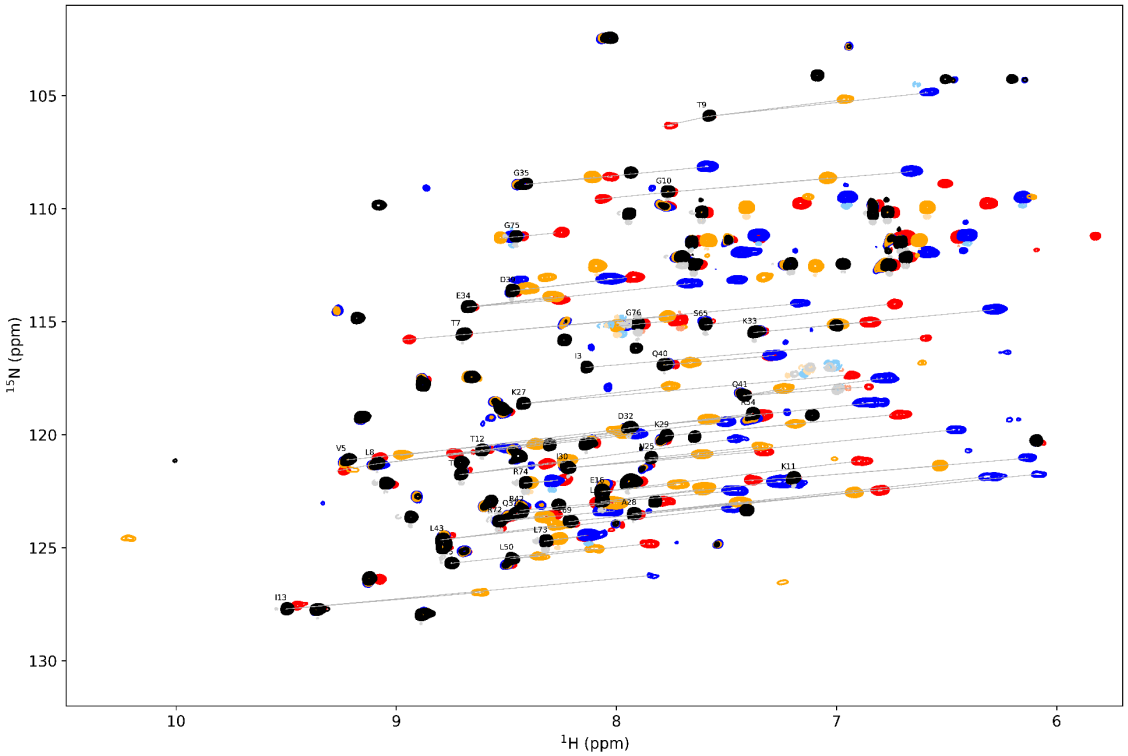

Figure S7: Overlay of ^{1}H-^{15}N HSQC spectra of Tm- (red, number of scans = 40), Dy- (blue, number of scans = 100), Tb- (orange, number of scans = 80) and Lu-M7-Nitro-Ub^{S57C} (black, number of scans = 24).

Overlay of ^{1}H-^{15}N HSQC spectra of Tm- (red), Dy- (blue), Tb- (orange), Yb- (green) and Lu-M7-Nitro (black) attached to selectively ^{15}N leucine labelled hCA II S50C

Measured in 10 mM phosphate buffer with pH 6.8 at a temperature of 298 K on a 600 MHz Bruker Avance III NMR spectrometer equipped with a cryogenic QCI-F probe.

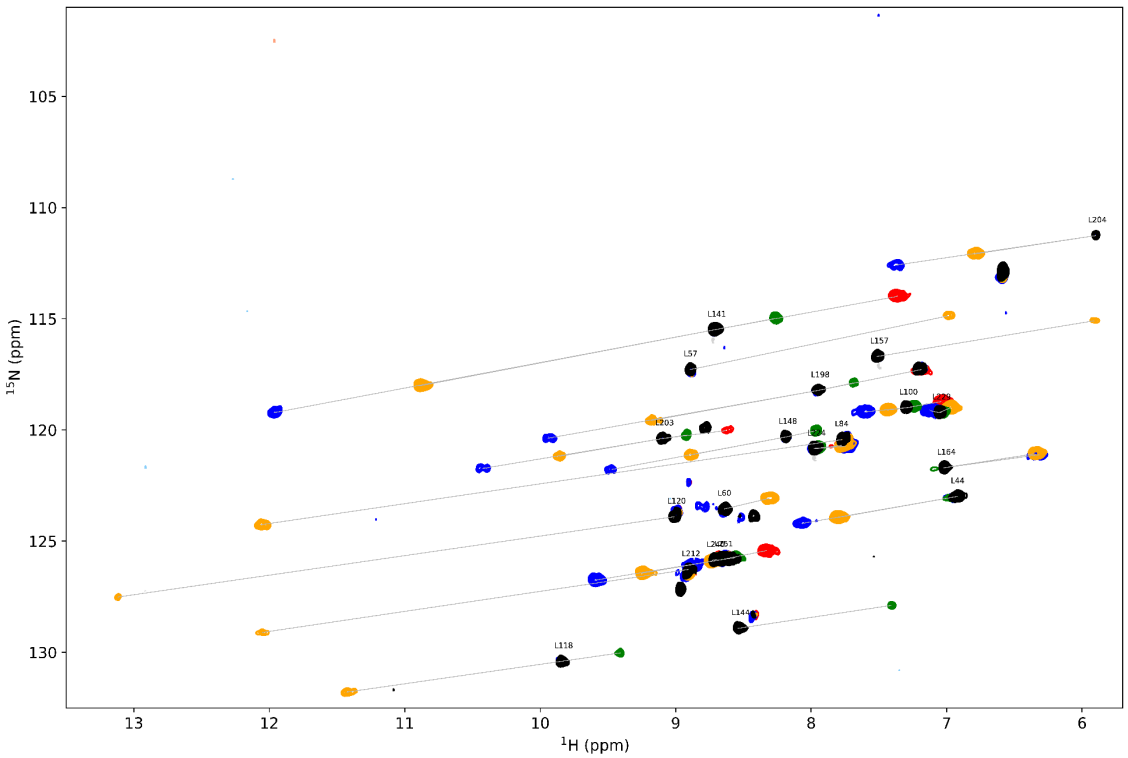

Figure S8: Overlay of ^{1}H-^{15}N HSQC spectra of Tm- (red, number of scans = 240), Dy- (blue, number of scans = 288), Tb- (orange, number of scans = 160), Yb- (green, number of scans = 136) and Lu-M7-Nitro (black, number of scans = 72) attached to selectively ^{15}N leucine labelled hCA II S50C.

Shift list comparison of ^{1}H-^{15}N HSQC spectra of Tm- and Lu-M7-Nitro-Ub^{S57C}

Table S3: Shift list comparison of ^{1}H-^{15}N HSQC spectra of Tm- and Lu-M7-Nitro-Ub^{S57C}.

Reson. 1	Residue	Shift Tm	Shift Lu	ΔPCS	RACS	Reson. 2	Residue	Shift Tm	Shift Lu	ΔPCS	RACS
H	3Ile	6.62	8.14	-1.52	0.002	N	3Ile	115.74	117.03	-1.29	0.017
H	5Val	9.10	9.22	-0.12	0.008	N	5Val	120.99	121.11	-0.12	-0.073
H	7Thr	8.97	8.70	0.27	0.008	N	7Thr	115.80	115.57	0.23	-0.099
H	12Thr	8.77	8.61	0.15	0.003	N	12Thr	120.85	120.69	0.16	-0.006
H	14Thr	8.35	8.71	-0.36	0.003	N	14Thr	121.30	121.77	-0.48	-0.027
H	16Glu	6.92	8.07	-1.15	-0.001	N	16Glu	121.19	122.52	-1.33	-0.081
H	27Lys	6.96	8.43	-1.46	0.003	N	27Lys	117.37	118.63	-1.26	0.024
H	28Ala	6.84	7.93	-1.09	-0.003	N	28Ala	122.47	123.50	-1.03	-0.058
H	29Lys	6.75	7.78	-1.03	0.007	N	29Lys	119.13	120.06	-0.93	-0.046
H	30Ile	7.36	8.22	-0.86	-0.002	N	30Ile	120.75	121.47	-0.72	0.002
H	32Asp	7.38	7.94	-0.57	0.001	N	32Asp	119.16	119.69	-0.53	-0.061
H	33Lys	6.88	7.38	-0.50	0.003	N	33Lys	115.03	115.48	-0.44	-0.064
H	34Glu	8.29	8.68	-0.39	-0.002	N	34Glu	114.05	114.36	-0.30	0.070
H	39Asp	7.95	8.48	-0.53	0.005	N	39Asp	113.05	113.65	-0.60	-0.002
H	40Gln	7.33	7.79	-0.46	-0.003	N	40Gln	116.54	116.92	-0.38	0.059
H	41Gln	6.89	7.42	-0.54	-0.006	N	41Gln	117.90	118.28	-0.38	0.050

Shift list comparison of ^{1}H-^{15}N HSQC spectra of Dy- and Lu-M7-Nitro-Ub^{S57C}

Table S4: Shift list comparison of ^{1}H-^{15}N HSQC spectra of Dy- and Lu-M7-Nitro-Ub^{S57C}.

Reson. 1	Residue	Shift Dy	Shift Lu	ΔPCS	RACS	Reson. 2	Residue	Shift Dy	Shift Lu	ΔPCS	RACS
H	7Thr	7.18	8.70	-1.52	-0.013	N	7Thr	114.21	115.57	-1.37	0.251
H	12Thr	7.51	8.61	-1.11	-0.007	N	12Thr	119.43	120.69	-1.26	-0.010
H	13Ile	7.85	9.50	-1.65	-0.005	N	13Ile	126.24	127.71	-1.47	0.099
H	14Thr	7.46	8.71	-1.25	0.003	N	14Thr	120.18	121.77	-1.59	-0.124
H	28Ala	6.32	7.93	-1.60	0.013	N	28Ala	121.86	123.50	-1.64	-0.094
H	30Ile	6.47	8.22	-1.75	0.004	N	30Ile	119.79	121.47	-1.68	-0.072
H	32Asp	6.85	7.94	-1.10	0.005	N	32Asp	118.60	119.69	-1.08	-0.061
H	33Lys	6.28	7.38	-1.09	0.002	N	33Lys	114.47	115.48	-1.01	0.031
H	34Glu	7.67	8.68	-1.00	-0.000	N	34Glu	113.33	114.36	-1.03	-0.113
H	39Asp	8.03	8.48	-0.45	-0.002	N	39Asp	113.12	113.65	-0.53	-0.068
H	40Gln	7.28	7.79	-0.50	-0.000	N	40Gln	116.50	116.92	-0.43	-0.034
H	41Gln	6.79	7.42	-0.64	0.007	N	41Gln	117.52	118.28	-0.76	-0.068
H	42Arg	7.47	8.44	-0.97	0.006	N	42Arg	122.49	123.34	-0.86	-0.023
H	43Leu	7.47	8.80	-1.33	-0.001	N	43Leu	123.24	124.65	-1.41	0.076
H	69Leu	6.09	8.22	-2.12	-0.004	N	69Leu	121.75	123.84	-2.09	0.125
H	71Leu	7.27	8.07	-0.80	0.009	N	71Leu	122.08	122.96	-0.88	-0.053

Shift list comparison of ^{1}H-^{15}N HSQC spectra of Tb- and Lu-M7-Nitro-Ub^{S57C}

Table S5: Shift list comparison of ^{1}H-^{15}N HSQC spectra of Tb- and Lu-M7-Nitro-Ub^{S57C}.

Reson. 1	Residue	Shift Tb	Shift Lu	ΔPCS	RACS	Reson. 2	Residue	Shift Tb	Shift Lu	ΔPCS	RACS
H	5Val	7.98	9.22	-1.25	-0.008	N	5Val	119.91	121.11	-1.21	0.120
H	7Thr	7.77	8.70	-0.93	-0.010	N	7Thr	114.77	115.57	-0.80	0.176
H	12Thr	7.96	8.61	-0.65	-0.005	N	12Thr	119.81	120.69	-0.88	-0.002
H	13Ile	8.61	9.50	-0.89	-0.003	N	13Ile	126.97	127.71	-0.74	0.089
H	14Thr	8.23	8.71	-0.48	-0.000	N	14Thr	121.22	121.77	-0.55	-0.054
H	15Leu	8.11	8.75	-0.64	0.007	N	15Leu	125.03	125.69	-0.66	-0.055
H	16Glu	7.73	8.07	-0.34	0.005	N	16Glu	122.21	122.52	-0.30	0.010
H	25Asn	7.35	7.85	-0.49	-0.002	N	25Asn	120.52	121.02	-0.50	-0.014
H	27Lys	7.76	8.43	-0.66	-0.002	N	27Lys	117.87	118.63	-0.76	-0.084
H	28Ala	7.45	7.93	-0.48	0.008	N	28Ala	122.98	123.50	-0.52	-0.025
H	29Lys	7.19	7.78	-0.59	-0.004	N	29Lys	119.54	120.06	-0.52	0.016
H	30Ile	7.61	8.22	-0.61	0.003	N	30Ile	120.87	121.47	-0.60	-0.040
H	31Gln	8.02	8.47	-0.44	0.003	N	31Gln	123.03	123.53	-0.51	-0.063
H	32Asp	7.59	7.94	-0.36	0.002	N	32Asp	119.33	119.69	-0.36	-0.002
H	33Lys	7.00	7.38	-0.37	-0.001	N	33Lys	115.13	115.48	-0.34	0.049
H	34Glu	8.30	8.68	-0.38	0.001	N	34Glu	113.91	114.36	-0.45	-0.091
H	39Asp	8.41	8.48	-0.07	-0.003	N	39Asp	113.55	113.65	-0.10	-0.025
H	40Gln	7.67	7.79	-0.12	0.000	N	40Gln	116.82	116.92	-0.10	-0.033
H	41Gln	7.25	7.42	-0.18	0.007	N	41Gln	117.97	118.28	-0.31	-0.061
H	43Leu	8.28	8.80	-0.52	0.001	N	43Leu	124.03	124.65	-0.62	0.033
H	69Leu	6.92	8.22	-1.29	-0.003	N	69Leu	122.56	123.84	-1.28	0.067
H	71Leu	7.61	8.07	-0.46	0.008	N	71Leu	122.41	122.96	-0.56	-0.073

Shift list comparison of ^{1}H-^{15}N HSQC spectra of Tm- and Lu-M7-Nitro attached to selectively ^{15}N leucine labelled hCA II S50C

Table S6: Shift list comparison of ^{1}H-^{15}N HSQC spectra of Tm- and Lu-M7-Nitro attached to selectively ^{15}N leucine labelled hCA II S50C.

Reson. 1	Residue	Shift Tm	Shift Lu	ΔPCS	RACS	Reson. 2	Residue	Shift Tm	Shift Lu	ΔPCS	RACS
H	100Leu	7.04	7.30	-0.26	-0.002	N	100Leu	118.73	119.01	-0.28	-0.092
H	141Leu	7.37	8.72	-1.35	0.004	N	141Leu	114.00	115.50	-1.50	0.006
H	198Leu	7.18	7.95	-0.77	0.000	N	198Leu	117.28	118.23	-0.94	-0.076
H	203Leu	8.63	9.10	-0.47	-0.002	N	203Leu	120.03	120.39	-0.36	0.077
H	251Leu	8.34	8.66	-0.33	0.002	N	251Leu	125.43	125.84	-0.40	-0.097

Shift list comparison of ^{1}H-^{15}N HSQC spectra of Dy- and Lu-M7-Nitro attached to selectively ^{15}N leucine labelled hCA II S50C

Table S7: Shift list comparison of ^{1}H-^{15}N HSQC spectra of Dy- and Lu-M7-Nitro attached to selectively ^{15}N leucine labelled hCA II S50C.

Reson. 1	Residue	Shift Dy	Shift Lu	ΔPCS	RACS	Reson. 2	Residue	Shift Dy	Shift Lu	ΔPCS	RACS
H	44Leu	8.07	6.92	1.15	0.010	N	44Leu	124.20	122.99	1.22	-0.073
H	100Leu	7.60	7.30	0.30	0.008	N	100Leu	119.19	119.01	0.18	-0.011
H	141Leu	11.96	8.72	3.25	-0.007	N	141Leu	119.22	115.50	3.72	0.171
H	148Leu	9.47	8.19	1.28	-0.014	N	148Leu	121.78	120.32	1.46	0.245
H	164Leu	6.32	7.02	-0.70	-0.004	N	164Leu	121.12	121.70	-0.59	0.073
H	198Leu	9.94	7.95	1.99	0.008	N	198Leu	120.37	118.23	2.15	-0.008
H	203Leu	10.42	9.10	1.32	-0.005	N	203Leu	121.73	120.39	1.34	0.058
H	204Leu	7.37	5.91	1.47	0.004	N	204Leu	112.59	111.27	1.32	-0.036
H	224Leu	7.75	7.98	-0.23	-0.002	N	224Leu	120.74	120.84	-0.11	0.062
H	229Leu	7.12	7.06	0.06	0.011	N	229Leu	119.14	119.22	-0.09	-0.092
H	251Leu	9.59	8.66	0.93	0.009	N	251Leu	126.75	125.84	0.92	-0.060

Shift list comparison of ^{1}H-^{15}N HSQC spectra of Tb- and Lu-M7-Nitro attached to selectively ^{15}N leucine labelled hCA II S50C

Table S8: Shift list comparison of ^{1}H-^{15}N HSQC spectra of Tb- and Lu-M7-Nitro attached to selectively ^{15}N leucine labelled hCA II S50C.

Reson. 1	Residue	Shift Tb	Shift Lu	ΔPCS	RACS	Reson. 2	Residue	Shift Tb	Shift Lu	ΔPCS	RACS
H	44Leu	7.80	6.92	0.89	0.007	N	44Leu	123.94	122.99	0.95	-0.060
H	57Leu	6.99	8.89	-1.90	-0.002	N	57Leu	114.88	117.29	-2.41	-0.008
H	60Leu	8.31	8.64	-0.33	0.003	N	60Leu	123.08	123.55	-0.48	-0.134
H	84Leu	12.06	7.77	4.28	-0.005	N	84Leu	124.26	120.44	3.82	0.057
H	100Leu	7.44	7.30	0.14	0.003	N	100Leu	119.11	119.01	0.10	0.035
H	118Leu	11.43	9.85	1.58	0.006	N	118Leu	131.79	130.41	1.38	-0.119
H	120Leu	13.12	9.01	4.11	0.009	N	120Leu	127.51	123.90	3.61	-0.097
H	141Leu	10.89	8.72	2.17	-0.006	N	141Leu	118.02	115.50	2.52	0.123
H	148Leu	8.90	8.19	0.71	-0.009	N	148Leu	121.13	120.32	0.81	0.166
H	157Leu	5.91	7.51	-1.60	0.002	N	157Leu	115.09	116.70	-1.61	-0.037
H	164Leu	6.35	7.02	-0.67	-0.001	N	164Leu	121.07	121.70	-0.63	0.029
H	198Leu	9.18	7.95	1.23	0.003	N	198Leu	119.57	118.23	1.35	0.038
H	203Leu	9.85	9.10	0.75	-0.004	N	203Leu	121.18	120.39	0.79	0.050
H	204Leu	6.78	5.91	0.88	0.001	N	204Leu	112.08	111.27	0.81	-0.011
H	212Leu	12.05	8.90	3.15	0.004	N	212Leu	129.11	126.27	2.83	-0.134
H	224Leu	7.78	7.98	-0.20	-0.001	N	224Leu	120.70	120.84	-0.15	0.007
H	229Leu	6.97	7.06	-0.09	0.009	N	229Leu	119.00	119.22	-0.22	-0.095
H	240Leu	8.74	8.72	0.01	0.001	N	240Leu	125.91	125.86	0.05	0.018
H	251Leu	9.25	8.66	0.59	0.006	N	251Leu	126.44	125.84	0.61	-0.025

Shift list comparison of ^{1}H-^{15}N HSQC spectra of Yb- and Lu-M7-Nitro attached to selectively ^{15}N leucine labelled hCA II S50C

Table S9: Shift list comparison of ^{1}H-^{15}N HSQC spectra of Yb- and Lu-M7-Nitro attached to selectively ^{15}N leucine labelled hCA II S50C.

Reson. 1	Residue	Shift Yb	Shift Lu	ΔPCS	RACS	Reson. 2	Residue	Shift Yb	Shift Lu	ΔPCS	RACS
H	100Leu	7.24	7.30	-0.06	-0.001	N	100Leu	118.96	119.01	-0.05	-0.016
H	118Leu	9.41	9.85	-0.43	-0.001	N	118Leu	130.03	130.41	-0.38	0.020
H	141Leu	8.27	8.72	-0.45	0.001	N	141Leu	114.99	115.50	-0.51	-0.007
H	144Leu	7.41	8.54	-1.13	-0.001	N	144Leu	127.89	128.92	-1.03	0.025
H	148Leu	7.97	8.19	-0.22	0.002	N	148Leu	120.04	120.32	-0.28	-0.034
H	198Leu	7.69	7.95	-0.26	-0.000	N	198Leu	117.89	118.23	-0.34	-0.014
H	203Leu	8.92	9.10	-0.18	-0.000	N	203Leu	120.23	120.39	-0.16	0.012
H	224Leu	7.96	7.98	-0.02	0.001	N	224Leu	120.81	120.84	-0.03	-0.011
H	229Leu	7.04	7.06	-0.01	-0.001	N	229Leu	119.22	119.22	0.00	0.015
H	240Leu	8.70	8.72	-0.03	0.001	N	240Leu	125.82	125.86	-0.04	-0.010
H	251Leu	8.56	8.66	-0.10	-0.001	N	251Leu	125.75	125.84	-0.09	-0.004

Residual dipolar couplings measured in ^{1}H-^{15}N HSQC spectra of Tm- and Lu-M7-Nitro-Ub^{S57C}

Table S10: Residual dipolar couplings measured in ^{1}H-^{15}N HSQC spectra of Tm- and Lu-M7-Nitro-Ub^{S57C}.

Residue	RDC (Hz)
3	-5.3
5	-18.9
7	-15.0
12	-5.7
14	-11.8
16	-14.8
27	0.3
28	8.1
29	-13.2
30	-4.2
32	1.7
33	-11.4
34	3.0
39	-4.9
40	-8.4
41	26.4
70	25.7

Residual dipolar couplings measured in ^{1}H-^{15}N HSQC spectra of Dy- and Lu-M7-Nitro-Ub^{S57C}

Table S11: Residual dipolar couplings measured in ^{1}H-^{15}N HSQC spectra of Dy- and Lu-M7-Nitro-Ub^{S57C}.

Residue	RDC (Hz)
7	41.3
12	20.2
13	33.1
14	-16.7
28	-20.0
30	-7.4
32	-30.3
33	-11.3
34	-0.2
39	-25.6
40	18.2
41	-28.7
43	-5.3
69	23.1
71	-25.8

Residual dipolar couplings measured in ^{1}H-^{15}N HSQC spectra of Tb- and Lu-M7-Nitro-Ub^{S57C}

Table S12: Residual dipolar couplings measured in ^{1}H-^{15}N HSQC spectra of Tb- and Lu-M7-Nitro-Ub^{S57C}.

Residue	RDC (Hz)
5	13.4
7	28.5
12	12.3
13	25.7
14	-2.6
15	-8.9
16	-2.9
27	-2.7
28	-16.7
29	-5.9
30	-6.3
31	-16.4
32	-15.3
33	0.5
34	-8.9
39	-11.2
40	16.0
41	-35.9
43	-11.9
69	8.9
71	-29.1

Residual dipolar couplings measured in ^{1}H-^{15}N HSQC spectra of Tb- and Lu-M7-Nitro attached to selectively ^{15}N leucine labelled hCA II S50C

Table S13: Residual dipolar couplings measured in ^{1}H-^{15}N HSQC spectra of Tb- and Lu-M7-Nitro attached to selectively ^{15}N leucine labelled hCA II S50C.

Residue	RDC (Hz)
44	-11.9
57	19.4
60	-24.7
84	31.2
100	-5.7
118	-23.4
120	-28.9
141	25.3
148	32.6
157	-19.2
164	-11.5
203	15.4
204	-9.3
212	-23.7
224	12.9
229	-29.5
240	-0.3
251	-16.1

Residual dipolar couplings measured in ^{1}H-^{15}N HSQC spectra of Yb- and Lu-M7-Nitro attached to selectively ^{15}N leucine labelled hCA II S50C

Table S14: Residual dipolar couplings measured in ^{1}H-^{15}N HSQC spectra of Yb- and Lu-M7-Nitro attached to selectively ^{15}N leucine labelled hCA II S50C.

Residue	RDC (Hz)
100	-0.7
118	4.7
141	-3.7
144	9.9
148	-2.5
198	0.0
203	-2.1
224	-4.1
229	4.9
240	-0.8
251	0.6

Paramagnetic relaxation enhancements measured in ^{1}H-^{15}N HSQC spectra of Gd- and Lu-M7-Nitro-Ub^{S57C}

Table S15: Paramagnetic relaxation enhancements measured in ^{1}H-^{15}N HSQC spectra of Gd- and Lu-M7-Nitro-Ub^{S57C}.

Residue	Intensity Lu	Intensity Gd	I_{para}/I_{dia} normalized to most distant residue (G76)	Distance to metal centre (Å)
3	86917	0	0.000	18.3
4	94962	49663	0.638	17.7
5	118292	63267	0.653	21.5
6	118676	79359	0.816	21.3
7	155439	115477	0.906	25.8
8	113994	84898	0.909	27.7
9	82717	74156	1.094	29.6
10	152503	129880	1.039	29.3
11	166971	123292	0.901	29.3
12	133538	103833	0.949	27.9
13	104644	75178	0.877	24.4
14	123349	99493	0.984	25.0
15	89614	28104	0.383	20.7
16	174689	91380	0.638	21.4
17	109940	57837	0.642	17.4
18	88948	897	0.012	15.8
20	84887	0	0.000	12.3
21	123910	16036	0.158	13.3
23	80998	5762	0.087	15.4
25	99596	11761	0.144	18.7
27	96665	23125	0.292	20.1
28	167410	97737	0.712	22.3
29	125868	70722	0.686	22.5
30	126145	76504	0.740	23.1
32	145289	114151	0.959	26.9
33	145191	111764	0.939	27.3
34	139282	106794	0.936	28.4
35	84185	68028	0.986	29.8
36	98417	76456	0.948	29.3
39	218771	169435	0.945	28.1
40	126676	105357	1.015	28.2
41	103959	80099	0.940	26.2
44	135114	60234	0.544	18.9
47	103235	50773	0.600	16.4
49	135447	10434	0.094	17.2
50	87124	7731	0.108	16.9
51	76591	2863	0.046	15.0
52	120904	54823	0.553	18.7
54	92930	6823	0.090	15.2

55	47919	1214	0.031	11.2
56	91153	9201	0.123	11.5
57	69446	0	0.000	9.0
58	71597	1143	0.019	8.0
59	73233	0	0.000	7.7
60	123061	0	0.000	5.6
61	78265	0	0.000	7.4
62	74016	0	0.000	9.6
64	76036	1319	0.021	15.3
65	112207	16038	0.174	14.3
66	107603	49296	0.559	15.7
67	118374	46029	0.474	17.8
68	120869	50009	0.505	18.4
69	137858	84595	0.749	22.6
70	114833	67884	0.721	23.3
71	193450	147342	0.929	27.8
72	205409	142694	0.848	28.4
73	274191	206123	0.917	31.9
74	242431	199996	1.007	34.1
75	150933	132985	1.075	36.1
76	461149	377931	1.000	39.4

Paramagnetic relaxation enhancements measured in ^{1}H-^{15}N HSQC spectra of Gd- and Lu-M7-Nitro attached to ^{15}N labelled hCA II S50C

Table S16: Paramagnetic relaxation enhancements measured in ^{1}H-^{15}N HSQC spectra of Gd- and Lu-M7-Nitro attached to ^{15}N labelled hCA II S50C.

Residue	Intensity Lu	Intensity Gd	I_{para}/I_{dia} normalized to most distant residue (E238)	Distance to metal centre (Å)
22	74623	75321	1.051	39.5
23	62717	68511	1.138	38.8
25	61088	65436	1.116	38.0
26	72277	69445	1.001	37.4
27	79305	80715	1.060	35.1
28	58286	62625	1.119	34.2
29	23707	22619	0.994	31.4
31	33405	31774	0.991	29.1
33	46672	43983	0.981	29.8
34	68271	57928	0.884	31.3
35	51704	36232	0.730	31.1
37	88764	82797	0.971	32.9
40	89276	55918	0.652	28.7
41	40502	33931	0.873	25.1
43	95228	63021	0.689	25.5
54	60620	1819	0.031	8.9
56	41231	9283	0.234	14.7
57	38824	14620	0.392	18.9
59	50088	29173	0.607	24.1
62	23533	25004	1.107	29.3
66	26642	19352	0.756	26.3
67	30026	20875	0.724	25.3
69	54706	26419	0.503	20.7
70	45351	17564	0.403	19.0
71	42012	19688	0.488	17.3
72	47711	16093	0.351	19.6
74	77505	30089	0.404	18.0
75	27179	7556	0.290	16.5
81	62800	0	0.000	15.6
82	24552	4258	0.181	16.0
85	30999	11160	0.375	21.3
86	158273	54966	0.362	19.6
92	41724	16018	0.400	18.6
93	33642	16343	0.506	18.7
94	43742	20857	0.497	20.3
97	54850	53477	1.015	28.9
98	21431	17059	0.829	30.0
99	30406	30066	1.030	34.5

100	70619	71283	1.051	34.3
101	57928	61177	1.100	34.0
102	84379	80530	0.994	34.2
103	98626	94106	0.994	32.7
104	34876	34020	1.016	31.4
105	71130	63085	0.924	29.1
106	20623	19947	1.007	27.0
107	25101	23973	0.995	26.8
108	54494	49089	0.938	29.3
109	63981	51017	0.830	29.6
110	61568	53578	0.906	30.9
111	54948	48030	0.910	32.6
112	104955	105335	1.045	32.1
113	69674	57923	0.866	32.4
114	39693	36525	0.958	28.5
115	53452	44706	0.871	27.4
116	82317	65450	0.828	26.1
118	38099	19434	0.531	20.9
119	42069	21259	0.526	20.6
121	36114	17844	0.515	18.1
123	41133	16004	0.405	18.8
124	30000	13708	0.476	22.0
125	62107	24729	0.415	19.9
127	123116	55485	0.469	22.3
128	91008	55895	0.640	24.2
129	67718	42235	0.650	24.4
130	114626	79137	0.719	26.2
131	56161	31646	0.587	24.7
132	91109	64876	0.742	27.4
133	93306	68773	0.768	28.5
134	89308	69136	0.806	26.9
135	88403	71395	0.841	27.7
136	92563	73933	0.832	29.8
137	99502	83720	0.876	29.3
139	81587	63235	0.807	27.9
140	48472	41454	0.891	26.4
144	32326	1656	0.053	17.5
145	43193	18553	0.447	18.8
146	38143	22434	0.613	19.5
147	31606	16539	0.545	20.4
148	43719	24553	0.585	23.2
149	54227	29962	0.575	23.0
151	79568	50122	0.656	25.8
152	40412	27392	0.706	24.7

157	72866	43894	0.627	17.6
158	80638	36824	0.476	19.0
159	102909	43388	0.439	19.1
160	78076	36683	0.489	19.6
161	59362	28099	0.493	22.0
162	92800	53683	0.602	23.6
163	80712	38776	0.500	24.4
164	62629	41402	0.688	26.3
166	98815	81331	0.857	29.5
167	87995	81736	0.967	30.0
168	80262	68337	0.887	32.6
170	42870	41936	1.019	35.6
172	105550	89609	0.884	33.0
173	101695	88075	0.902	31.1
174	71073	52274	0.766	26.8
175	158562	113643	0.746	26.7
177	106445	43475	0.425	20.7
178	79473	27453	0.360	16.5
183	46980	0	0.000	10.4
184	53975	4085	0.079	11.8
185	81778	2353	0.030	11.5
188	50972	5327	0.109	14.9
189	66817	0	0.000	13.5
192	44522	22448	0.525	21.1
196	55783	42014	0.784	23.8
198	33247	28416	0.890	29.0
200	51206	53710	1.092	29.6
203	28423	27634	1.013	32.2
204	20166	16454	0.850	31.6
205	53457	44516	0.867	32.5
206	55938	43709	0.814	28.9
207	63655	55784	0.913	27.4
208	47268	25937	0.571	23.3
209	48486	32593	0.700	24.0
210	41455	19195	0.482	20.3
211	58309	31747	0.567	20.8
212	45310	23590	0.542	18.7
214	52087	28507	0.570	18.6
216	51491	18265	0.369	19.5
217	72034	28788	0.416	19.6
218	68393	38391	0.585	23.2
219	59106	38853	0.685	24.0
220	96015	70280	0.762	28.4
221	103591	78335	0.788	28.8

222	66193	51154	0.805	26.8
223	72891	49840	0.712	27.1
224	100679	78675	0.814	29.5
225	98132	81529	0.865	29.1
226	83982	63901	0.792	28.1
227	55840	46757	0.872	30.5
228	79371	80946	1.062	31.8
229	79067	77730	1.024	31.8
230	53307	46444	0.907	33.5
232	57520	56777	1.028	37.8
233	55337	56855	1.070	39.7
235	34026	34893	1.068	42.1
236	108892	111167	1.063	42.6
238	99806	95831	1.000	43.8
239	57104	58780	1.072	39.9
240	86884	76780	0.920	39.2
242	62157	64547	1.082	34.9
244	59564	57439	1.004	31.9
245	69199	67054	1.009	32.7
248	77481	68119	0.916	34.0
251	87598	88934	1.057	36.4
252	104976	102303	1.015	37.5
254	121797	115014	0.983	35.3
255	101304	83352	0.857	31.8
256	89030	77306	0.904	30.6
257	58471	45890	0.817	26.3
258	80508	49231	0.637	25.9
259	50401	18495	0.382	21.7
260	77598	42160	0.566	22.6
261	120162	70776	0.613	23.6

Residue-specific plots of experimental PRE onto the sequence of ubiquitin S57C and hCA S50C constructs

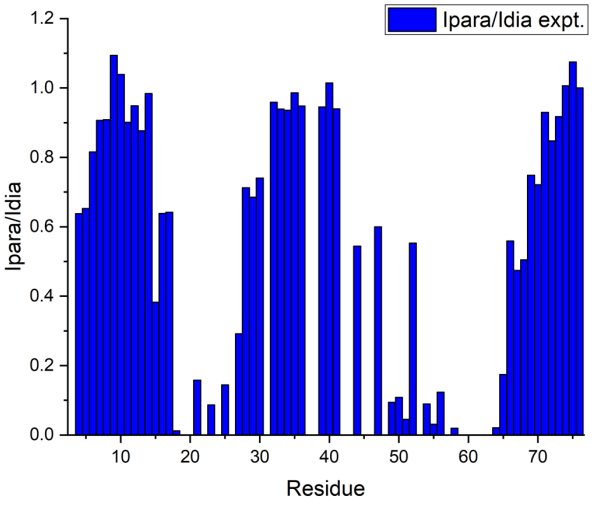

Figure S9: Residue-specific plot of experimental PRE detected on ^{15}N labelled ubiquitin S57C labelled with Gd-M7-Nitro.

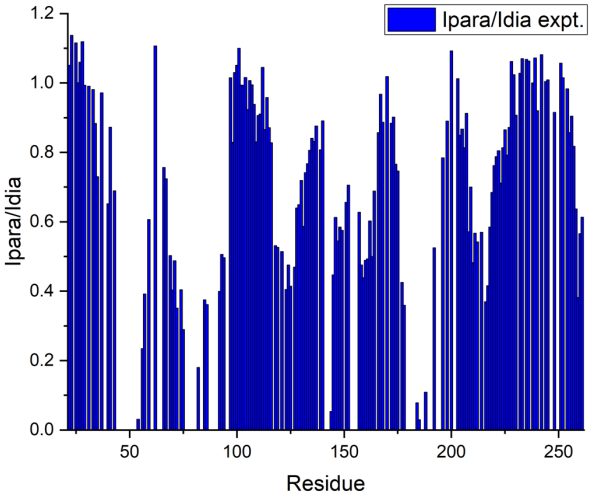

Figure S10: Residue-specific plot of experimental PRE detected on selectively ^{15}N labelled hCA S50C labelled with Gd-M7-Nitro.

Plots of experimental and calculated PRE for ubiquitin S57C and hCA S50C constructs

Theoretical PRE were calculated using the relation I_{para}/I_{dia}, $\frac{I_{para}}{I_{dia}} = \frac{R_2^{dia} \cdot \exp(-R_2^{para} \cdot t)}{R_2^{dia} + R_2^{para}}$ reported in literature.[1, 11]

While R_2^{dia} was determined from the linewidths of the diamagnetic sample ($R_2^{dia} = \pi \cdot \Delta\nu_{1/2}$), t is the INEPT delay (9 ms). R_2^{para} was substituted with the expression from the simplified Solomon-Bloembergen equation:[11]

$$R_2^{para} = \frac{1}{15}\left(\frac{\mu_0}{4\pi}\right)^2 \frac{\gamma_H^2 g^2 \mu_B^2 J(J+1)}{r^6}\left(4\tau_c + \frac{3\tau_c}{1+\omega_H^2\tau_c^2}\right)$$

yielding the complete function for calculation of I_{para}/I_{dia} for a given r:

$$\frac{I_{para}}{I_{dia}} = \frac{R_2^{dia} \cdot \exp\left(-\frac{1}{15}\left(\frac{\mu_0}{4\pi}\right)^2 \frac{\gamma_H^2 g^2 \mu_B^2 J(J+1)}{r^6}\left(4\tau_c + \frac{3\tau_c}{1+\omega_H^2\tau_c^2}\right) \cdot t\right)}{R_2^{dia} + \frac{1}{15}\left(\frac{\mu_0}{4\pi}\right)^2 \frac{\gamma_H^2 g^2 \mu_B^2 J(J+1)}{r^6}\left(4\tau_c + \frac{3\tau_c}{1+\omega_H^2\tau_c^2}\right)}$$

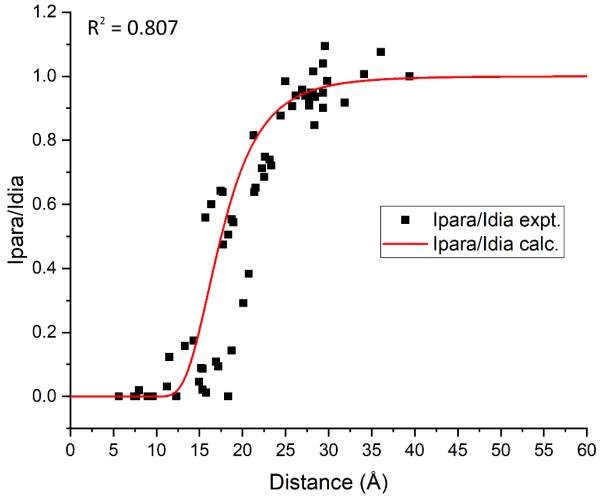

Figure S11: Plot of experimental and calculated PRE of ^{15}N labelled ubiquitin S57C labelled with Gd-M7-Nitro.

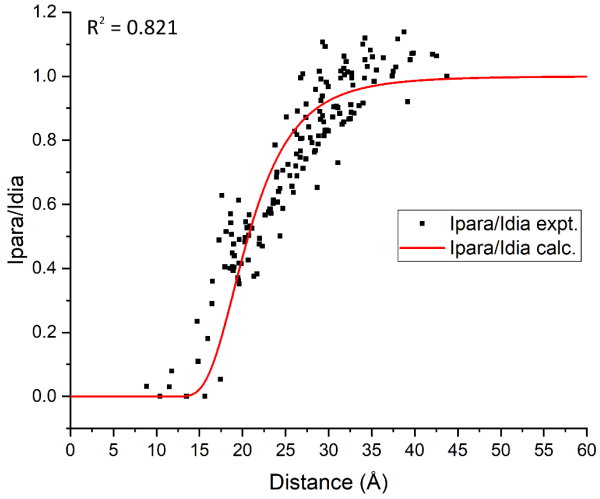

Figure S12: Plot of experimental and calculated PRE of selectively ^{15}N labelled hCA S50C labelled with Gd-M7-Nitro.

Correlation plots of experimental and back-calculated PCS and RDC

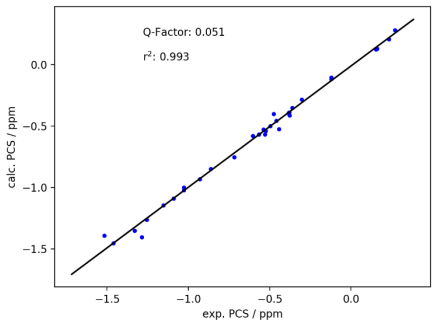

Figure S13: PCS correlation plot of ^{15}N labelled ubiquitin S57C labelled with Tm-M7-Nitro.

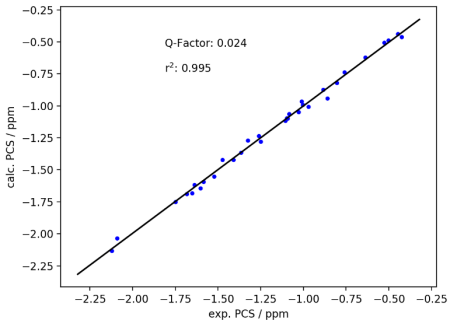

Figure S14: PCS correlation plot of ^{15}N labelled ubiquitin S57C labelled with Dy-M7-Nitro.

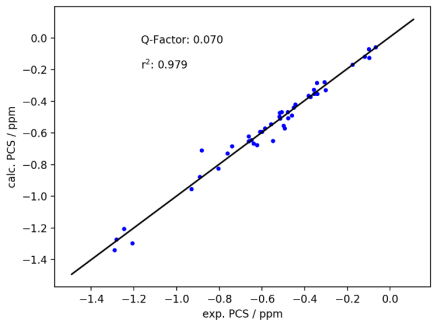

Figure S15: PCS correlation plot of ^{15}N labelled ubiquitin S57C labelled with Tb-M7-Nitro.

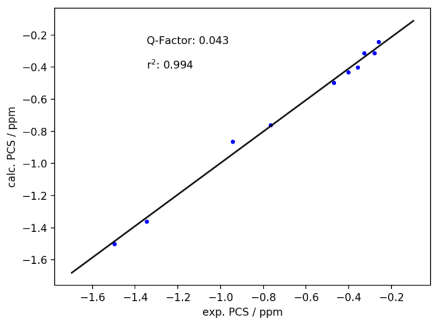

Figure S16: PCS correlation plot of selectively ^{15}N leucine labelled hCA S50C labelled with Tm-M7-Nitro.

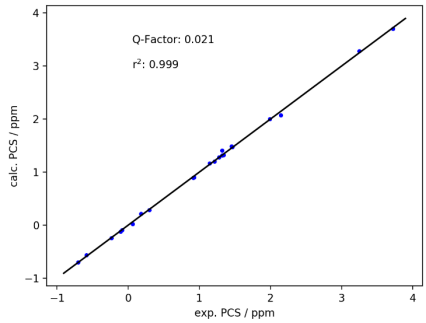

Figure S17: PCS correlation plot of selectively ^{15}N leucine labelled hCA S50C labelled with Dy-M7-Nitro.

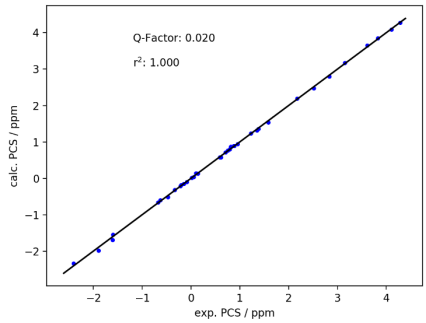

Figure S18: PCS correlation plot of selectively ^{15}N leucine labelled hCA S50C labelled with Tb-M7-Nitro.

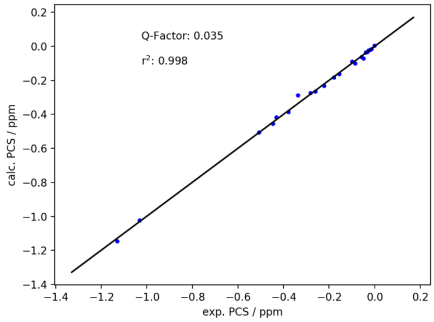

Figure S19: PCS correlation plot of selectively ^{15}N leucine labelled hCA S50C labelled with Yb-M7-Nitro.

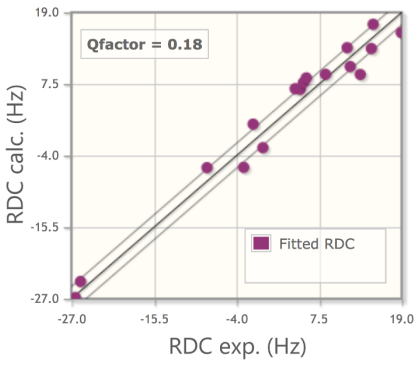

Figure S20: RDC correlation plot of ^{15}N labelled ubiquitin S57C labelled with Tm-M7-Nitro (graphics adapted from Fanten[9]).

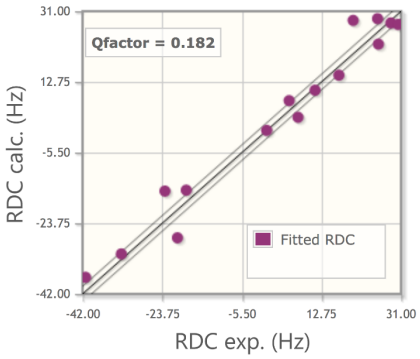

Figure S21: RDC correlation plot of ^{15}N labelled ubiquitin S57C labelled with Dy-M7-Nitro (graphics adapted from Fanten[9]).

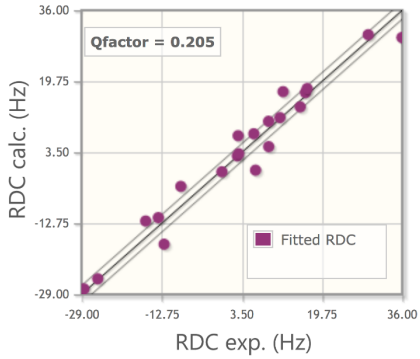

Figure S22: RDC correlation plot of ^{15}N labelled ubiquitin S57C labelled with Tb-M7-Nitro (graphics adapted from Fanten[9]).

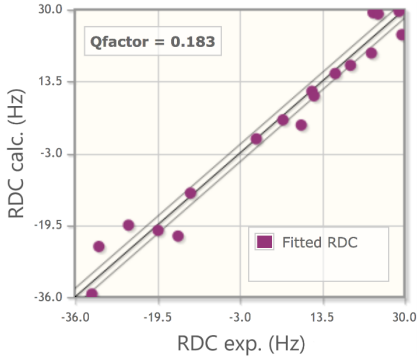

Figure S23: RDC correlation plot of selectively ^{15}N leucine labelled hCA S50C labelled with Tb-M7-Nitro (graphics adapted from Fanten[9]).

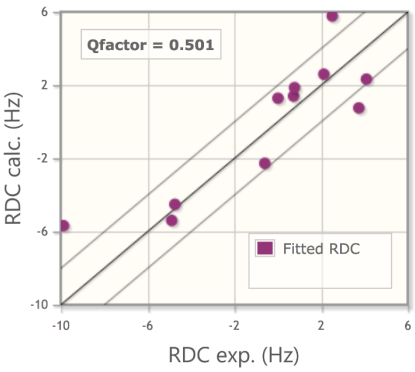

Figure S24: RDC correlation plot of selectively ^{15}N leucine labelled hCA S50C labelled with Yb-M7-Nitro (graphics adapted from Fanten[9]).

ESI-MS measurements of tagging reactions

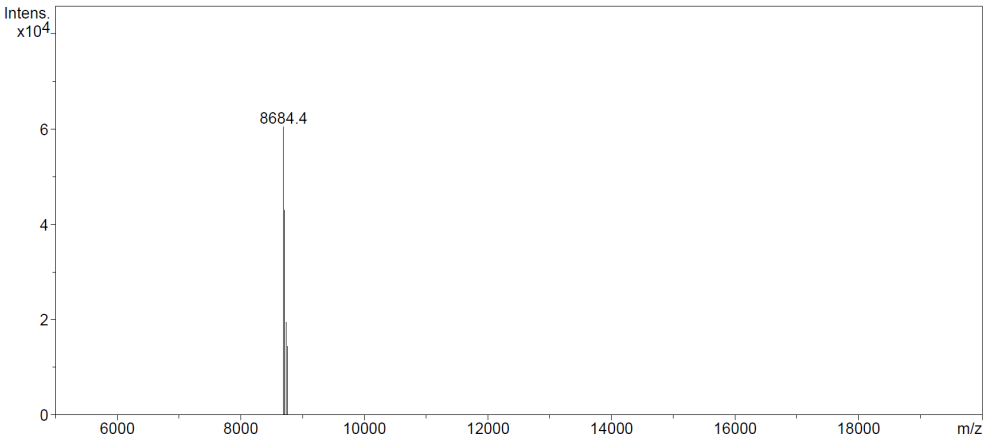

Figure S25: ESI-MS spectrum of ^{15}N labelled ubiquitin S57C.

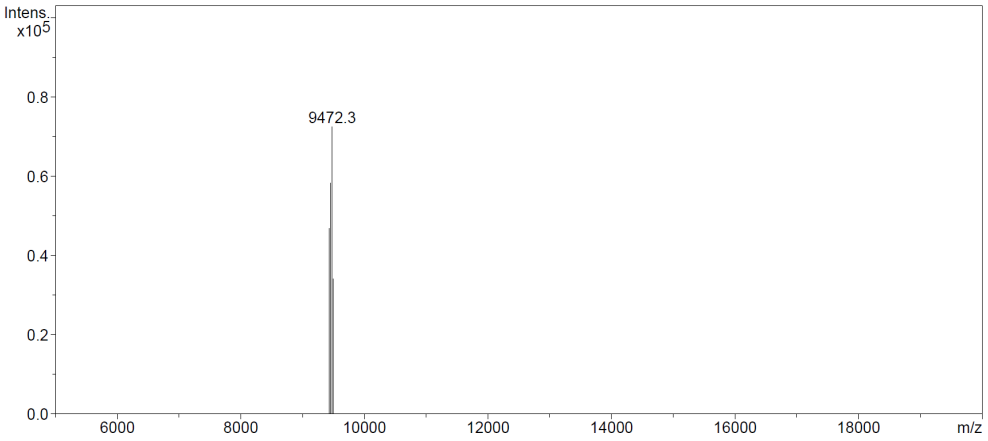

Figure S26: Confirmation of tagging reaction of ^{15}N labelled ubiquitin S57C with Tm-M7-Nitro monitored by ESI-MS.

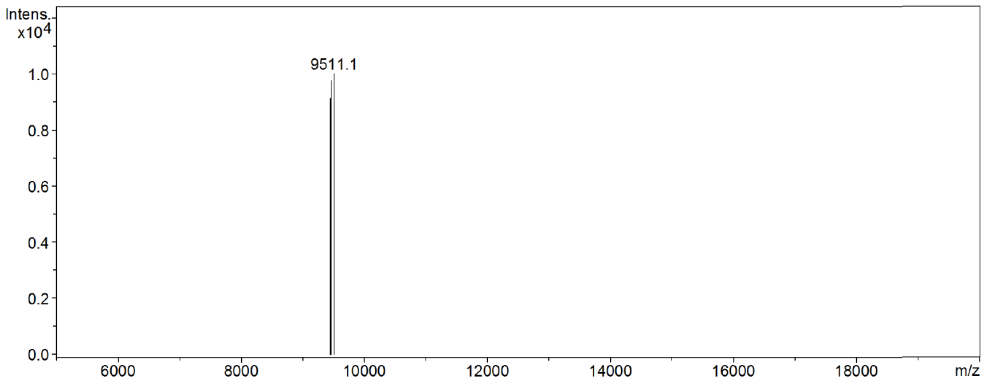

Figure S27: Confirmation of tagging reaction of ^{15}N labelled ubiquitin S57C with Dy-M7-Nitro monitored by ESI-MS.

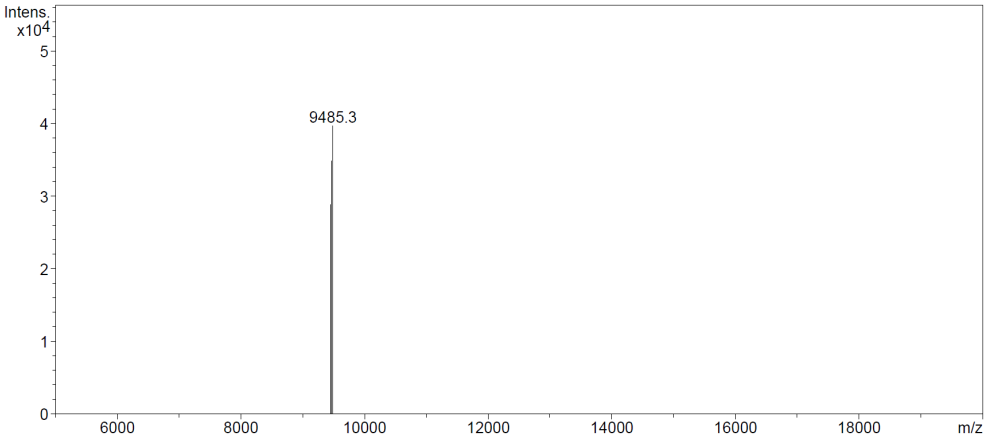

Figure S28: Confirmation of tagging reaction of ^{15}N labelled ubiquitin S57C with Tb-M7-Nitro monitored by ESI-MS.

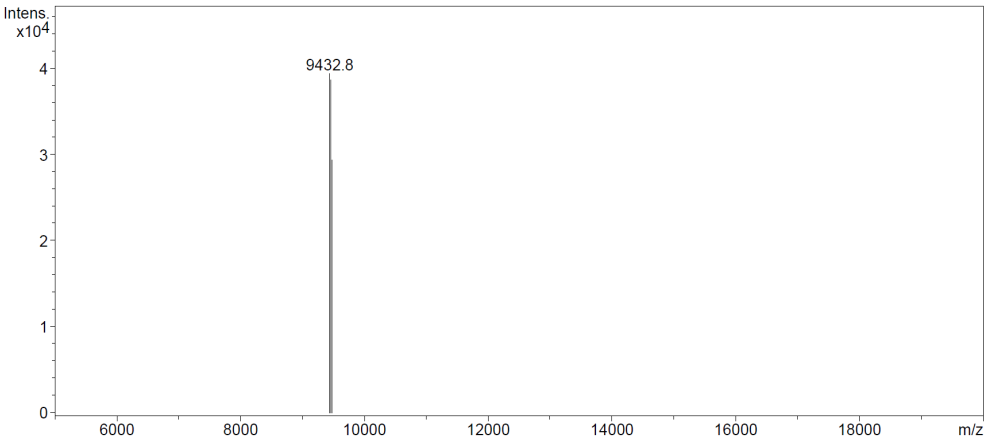

Figure S29: Confirmation of tagging reaction of ^{15}N labelled ubiquitin S57C with Lu-M7-Nitro monitored by ESI-MS.

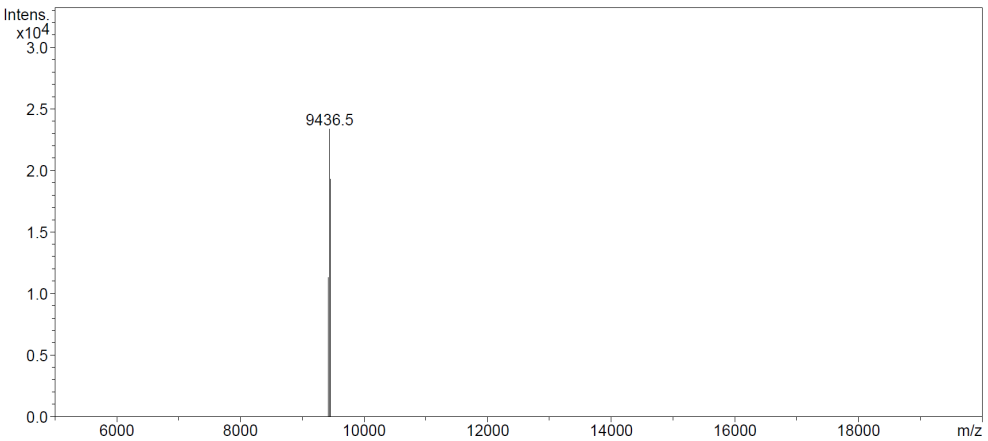

Figure S30: Confirmation of tagging reaction of ^{15}N labelled ubiquitin S57C with Gd-M7-Nitro monitored by ESI-MS.

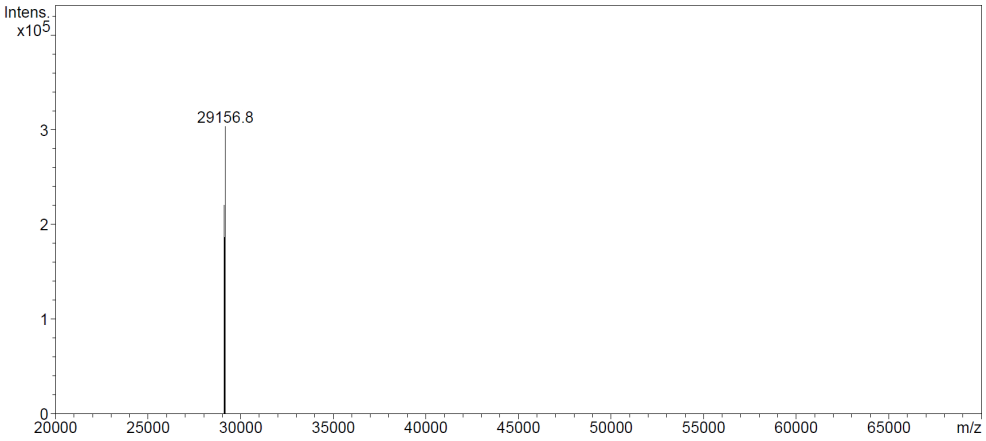

Figure S31: ESI-MS spectrum of selectively ^{15}N leucine labelled hCA II S50C.

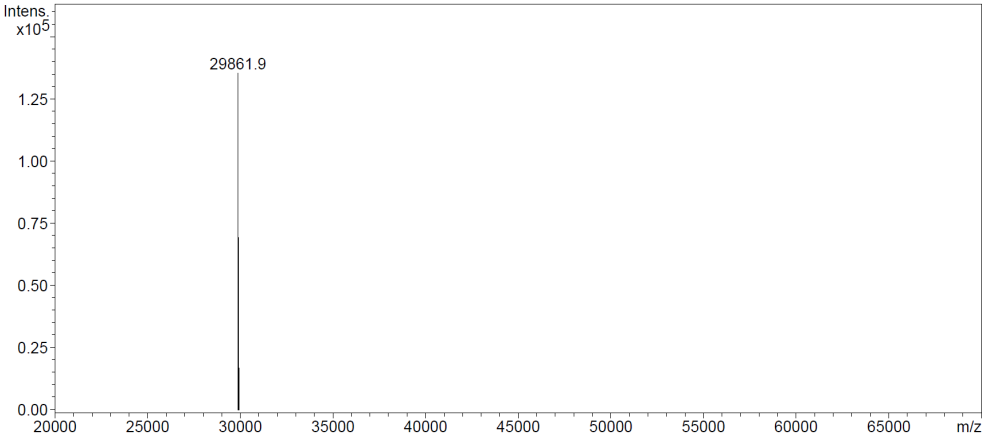

Figure S32: Confirmation of tagging reaction of selectively ^{15}N leucine labelled hCA II S50C with Tm-M7-Nitro monitored by ESI-MS.

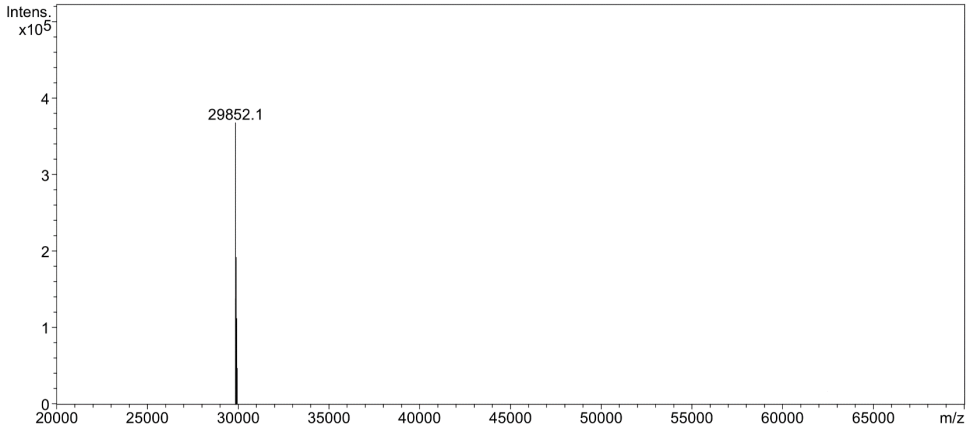

Figure S33: Confirmation of tagging reaction of selectively ^{15}N leucine labelled hCA II S50C with Dy-M7-Nitro monitored by ESI-MS.

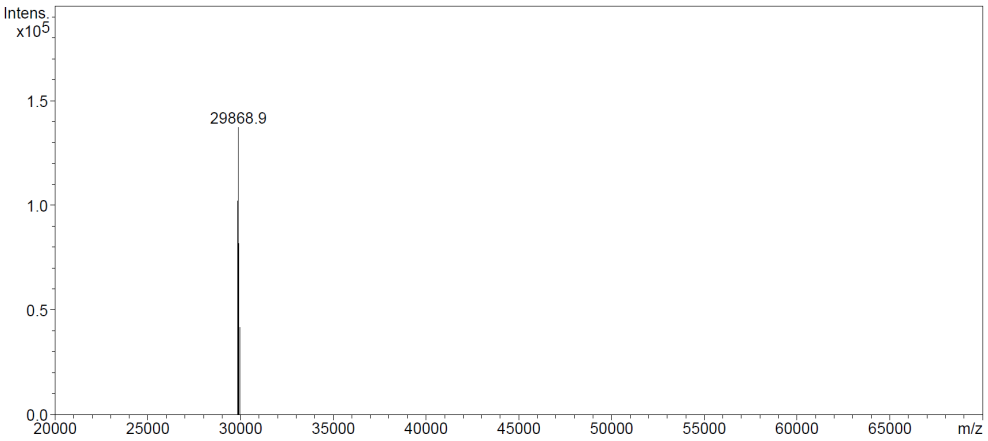

Figure S34: Confirmation of tagging reaction of selectively ^{15}N leucine labelled hCA II S50C with Tb-M7-Nitro monitored by ESI-MS.

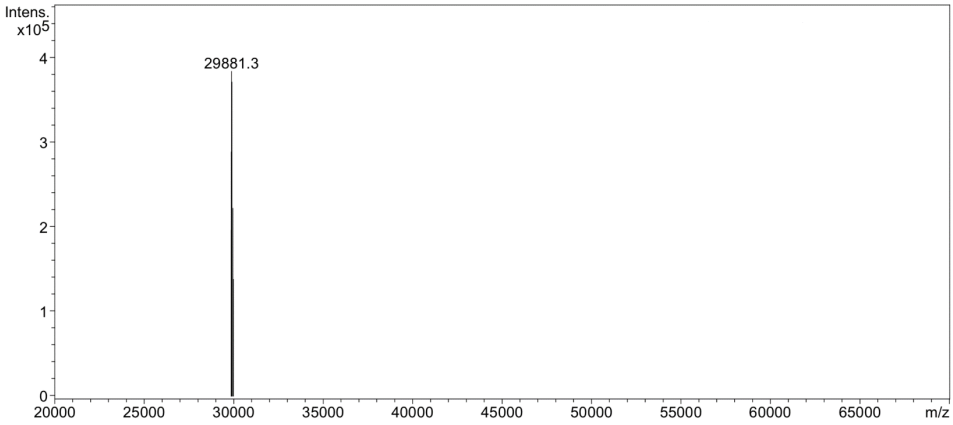

Figure S35: Confirmation of tagging reaction of selectively ^{15}N leucine labelled hCA II S50C with Yb-M7-Nitro monitored by ESI-MS.

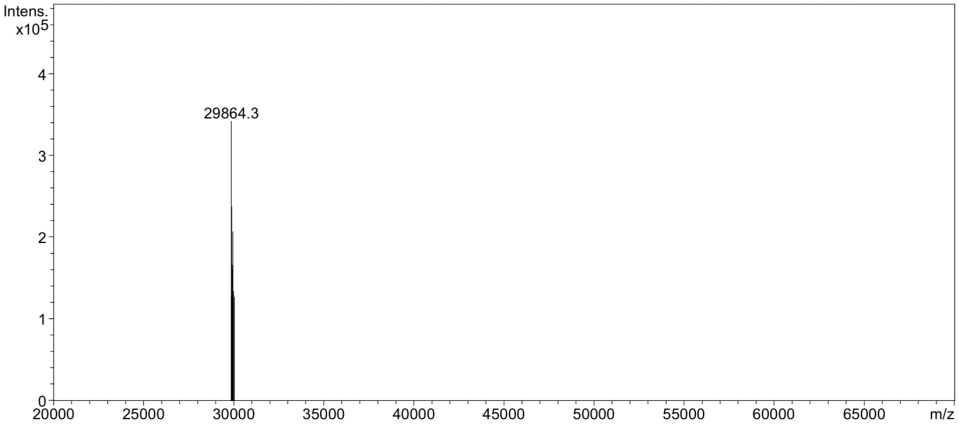

Figure S36: Confirmation of tagging reaction of selectively ^{15}N leucine labelled hCA II S50C with Lu-M7-Nitro monitored by ESI-MS.

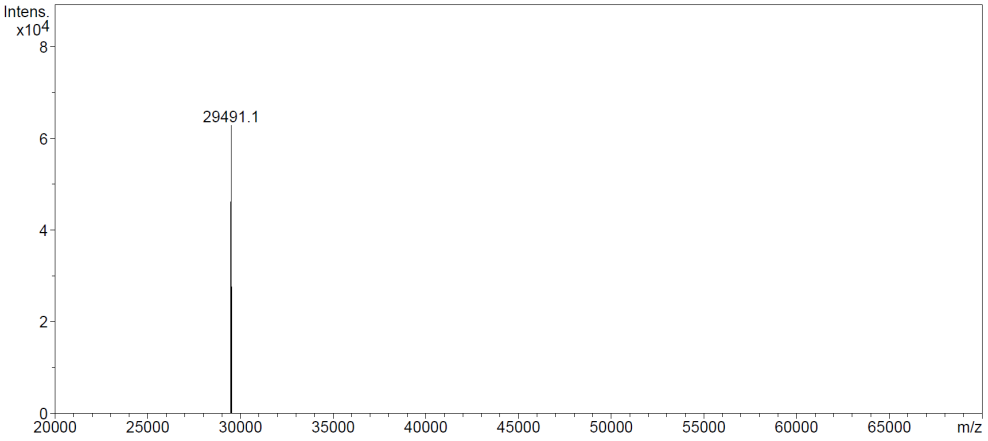

Figure S37: ESI-MS spectrum of uniformly ^{15}N labelled hCA II S50C.

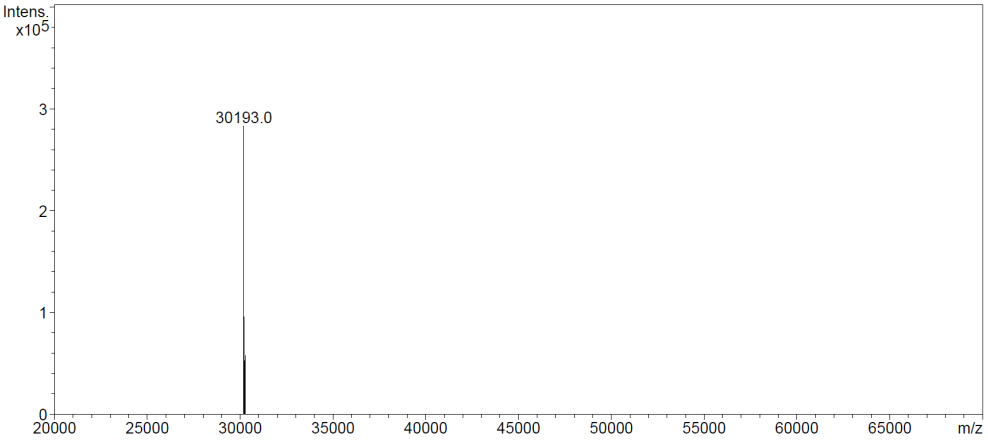

Figure S38: Confirmation of tagging reaction of uniformly ^{15}N labelled hCA II S50C with Lu-M7-Nitro monitored by ESI-MS.

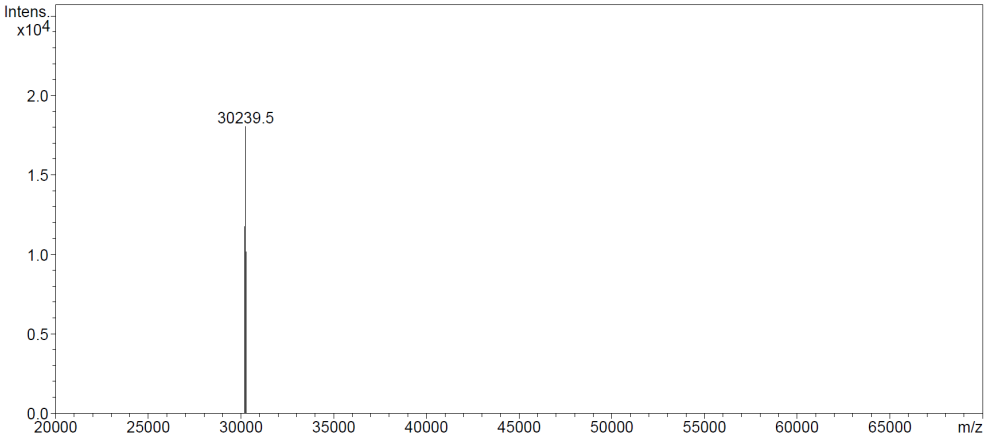

Figure S39: Confirmation of tagging reaction of uniformly ^{15}N labelled hCA II S50C with Gd-M7-Nitro monitored by ESI-MS.

Complete fitting results using Numbat, Paramagpy and Fanten

Table S17: Complete fitting results using Numbat[8], Paramagpy[10] and Fanten[9]. Induced axial and rhombic components of the paramagnetic susceptibility tensors ($\Delta\chi_{ax}$ and $\Delta\chi_{rh}$, in 10^{-32} m^3), metal position in PDB coordinate frame (X_{metal}, Y_{metal}, Z_{metal}, in Å), Euler angles (α, β, γ, in °) and quality factor (Q, mathematical definition in SI, p. 1) on ubiquitin S57C (pH 6.0) and selectively ^{15}N leucine labelled hCA II S50C (pH 6.8) at 298 K. Note: Numbat[8] and Paramagpy[10] yield anisotropy parameters in UTR convention, Fanten[9] depicts tensors in the Fanten convention. For RDC only fits, the metal position of the corresponding PCS fit was given.

Protein mutant + fitting routine	PDB	N° PCS	Ln^{3+}	$\Delta\chi_{ax}$ (10^{-32} m^3)	$\Delta\chi_{rh}$ (10^{-32} m^3)	X_{metal} (Å)	Y_{metal} (Å)	Z_{metal} (Å)	Distance to $C_{B,Cys}$ (Å)	α (°)	β (°)	γ (°)	Q (%)
UbiS57C Numbat	1UBI	32	Tm	60.9 ± 1.9	12.3 ± 1.3	16.3	16.9	12.3	6.9	110.9	70.4	101.4	5.1
		32	Dy	94.3 ± 2.2	10.7 ± 0.7					133.7	161.5	128.4	2.4
		44	Tb	65.9 ± 1.6	27.9 ± 0.8					128.0	162.4	110.4	7.0
UbiS57C Paramagpy	1UBI	32	Tm	73.3	17.9	15.8	16.1	11.9	7.4	112.4	68.2	100.6	5.1
		32	Dy	112.4	15.1					131.3	161.1	114.6	2.6
		44	Tb	79.5	34.9					125.2	162.2	104.6	7.2
UbiS57C Fanten	1UBI	32	Tm	64.5	-12.7	16.0	16.4	11.1	7.1	167.2	-112.6	112.1	6.1
		32	Dy	101.6	-9.7					153.2	-20.4	126.3	4.9
		44	Tb	72.8	-30.7					-171.8	-161.3	-61.6	10.1
UbiS57C Fanten jointly with RDC	1UBI	32	Tm	66.6	-12.5	14.2	17.4	13.4	9.2	164.0	-103.2	107.4	14.2
		32	Dy	106.7	-2.0					144.7	-164.8	-42.0	8.5
		44	Tb	78.8	-31.8					144	-15.4	144.5	19.3
hCA II S50C Numbat	3KS3	10	Tm	71.0 ± 1.8	6.2 ± 0.9	-31.0	4.4	14.9	7.1	174.7	17.4	139.0	4.3
		22	Dy	95.9 ± 1.1	13.1 ± 2.5					179.8	112.5	64.5	2.1
		38	Tb	63.6 ± 0.9	22.5 ± 1.4					4.9	62.5	109.5	2.0
		22	Yb	13.8 ± 0.6	7.5 ± 0.4					36.7	163.0	115.4	3.5
hCA II S50C Paramagpy	3KS3	10	Tm	89.2	13.5	-31.2	4.2	14.9	7.4	161.5	17.2	0.6	4.9
		22	Dy	98.2	17.3					1.1	67.5	114.9	2.5
		38	Tb	65.5	24.9					6.5	62.6	108.3	2.0
		22	Yb	14.4	7.7					38.4	162.0	115.8	3.6
hCA II S50C Fanten	3KS3	10	Tm	88.8	-21.6	-31.0	5.0	14.9	6.9	15.5	-121.0	-110.8	7.1
		22	Dy	97.4	-14.9					-17.7	-112.3	-2.5	4.5
		38	Tb	64.8	-22.4					-14.7	-116.9	2.6	3.1
		22	Yb	14.8	-7.1					14.3	-164.9	-156.7	4.6
hCA II S50C Fanten jointly with RDC	3KS3	10	Tm	102.5	-24.0	-31.6	6.5	15.4	6.6	10.2	-117.9	-111.0	7.4
		22	Dy	100.2	-23.1					20.6	-109.3	-8.0	4.5
		38	Tb	74.0	-23.4					-21.0	-112.7	-2.5	16.2
		22	Yb	14.1	-6.3					-125.6	-151.3	-123.6	14.0
Protein mutant + fitting routine	**PDB**	**N° RDC**	**Ln^{3+}**	**$\Delta\chi_{ax}$ (10^{-32} m^3)**	**$\Delta\chi_{rh}$ (10^{-32} m^3)**	**X_{metal} (Å)**	**Y_{metal} (Å)**	**Z_{metal} (Å)**	**Distance to $C_{B,Cys}$ (Å)**	**α (°)**	**β (°)**	**γ (°)**	**Q (%)**
UbiS57C Paramagpy	1UBI	17	Tm	59.7	11.8	15.8	16.1	11.9	7.4	107.4	76.8	105.7	18.0
		15	Dy	96.0	3.2					137.1	165.3	41.4	18.2
		21	Tb	71.3	29.3					146.2	164.3	126.8	20.5
UbiS57C Fanten	1UBI	17	Tm	66.3	-13.1	16.0	16.4	11.1	7.1	164.3	-103.2	107.4	18.0
		15	Dy	106.7	-3.5					-131.4	-14.7	137.1	18.2
		21	Tb	79.2	-32.5					143.2	-15.7	146.2	20.5
UbiS57C Fanten jointly with PCS	1UBI	17	Tm	66.6	-12.5	14.2	17.4	13.4	9.2	164.0	-103.2	107.4	18.1
		15	Dy	106.7	-19.9					144.7	-164.8	-42.0	18.3
		21	Tb	78.8	-31.8					144	-15.4	144.5	20.5
hCA II S50C Paramagpy	3KS3	18	Tb	67.4	21.0	-31.2	4.2	14.9	7.4	176.7	111.9	66.8	18.3
		11	Yb	12.5	5.4					56.7	151.1	143.6	50.1
hCA II S50C Fanten	3KS3	18	Tb	74.9	-23.3	-31.0	5.0	14.9	6.9	-23.2	-111.9	-3.3	18.3
		11	Yb	13.9	-6.0					-126.4	-151.1	-123.3	50.1
hCA II S50C Fanten jointly with PCS	3KS3	18	Tb	74.0	-23.4	-31.6	6.5	15.4	6.6	-21.0	-112.7	-2.5	18.5
		11	Yb	14.1	-6.3					-125.6	-151.3	-123.6	50.1

Fitting results using Fanten (PCS only, RDC only and PCS/RDC combined fits)

Table S18: Fitting results using Fanten[9] (PCS only and PCS/RDC combined fit). Induced axial and rhombic components of the paramagnetic susceptibility tensors ($\Delta\chi_{ax}$ and $\Delta\chi_{rh}$, in 10^{-32} m^3), metal position in PDB coordinate frame (X_{metal}, Y_{metal}, Z_{metal}, in Å), Euler angles (α, β, γ, in °) and quality factor (Q, mathematical definition in SI, p. 1) on ubiquitin S57C (pH 6.0) and selectively ^{15}N leucine labelled hCA II S50C (pH 6.8) at 298 K.

Protein mutant + fitting routine	PDB	N° PCS	Ln^{3+}	$\Delta\chi_{ax}$ (10^{-32} m^3)	$\Delta\chi_{rh}$ (10^{-32} m^3)	X_{metal} (Å)	Y_{metal} (Å)	Z_{metal} (Å)	Distance to $C_{\beta,Cys}$ (Å)	α (°)	β (°)	γ (°)	Q (%)
UbiS57C Fanten; PCS only	1UBI	32	Tm	64.5	-12.7	16.0	16.4	11.1	7.1	167.2	-112.6	112.1	6.1
		32	Dy	101.6	-9.7					153.2	-20.4	126.3	4.9
		44	Tb	72.8	-30.7					-171.8	-161.3	-61.6	10.1
UbiS57C Fanten; PCS jointly with RDC	1UBI	32	Tm	66.6	-12.5	14.2	17.4	13.4	9.2	164.0	-103.2	107.4	14.2
		32	Dy	106.7	-2.0					144.7	-164.8	-42.0	8.5
		44	Tb	78.8	-31.8					144	-15.4	144.5	19.3
hCA II S50C Fanten; PCS only	3KS3	10	Tm	88.8	-21.6	-31.0	5.0	14.9	6.9	15.5	-121.0	-110.8	7.1
		22	Dy	97.4	-14.9					-17.7	-112.3	-2.5	4.5
		38	Tb	64.8	-22.4					-14.7	-116.9	2.6	3.1
		22	Yb	14.8	-7.1					14.3	-164.9	-156.7	4.6
hCA II S50C Fanten; PCS jointly with RDC	3KS3	10	Tm	102.5	-24.0	-31.6	6.5	15.4	6.6	10.2	-117.9	-111.0	7.4
		22	Dy	100.2	-23.1					20.6	-109.3	-8.0	4.5
		38	Tb	74.0	-23.4					-21.0	-112.7	-2.5	16.2
		22	Yb	14.1	-6.3					-125.6	-151.3	-123.6	14.0
Protein mutant + fitting routine	**PDB**	**N° RDC**	**Ln^{3+}**	**$\Delta\chi_{ax}$ (10^{-32} m^3)**	**$\Delta\chi_{rh}$ (10^{-32} m^3)**	**X_{metal} (Å)**	**Y_{metal} (Å)**	**Z_{metal} (Å)**	**Distance to $C_{\beta,Cys}$ (Å)**	**α (°)**	**β (°)**	**γ (°)**	**Q (%)**
UbiS57C Fanten; RDC only	1UBI	17	Tm	66.3	-13.1	16.0	16.4	11.1	7.1	164.3	-103.2	107.4	18.0
		15	Dy	106.7	-3.5					-131.4	-14.7	137.1	18.2
		21	Tb	79.2	-32.5					143.2	-15.7	146.2	20.5
UbiS57C Fanten; RDC jointly with PCS	1UBI	17	Tm	66.6	-12.5	14.2	17.4	13.4	9.2	164.0	-103.2	107.4	18.1
		15	Dy	106.7	-19.9					144.7	-164.8	-42.0	18.3
		21	Tb	78.8	-31.8					144	-15.4	144.5	20.5
hCA II S50C Fanten; RDC	3KS3	18	Tb	74.9	-23.3	-31.0	5.0	14.9	6.9	-23.2	-111.9	-3.3	18.3
		11	Yb	13.9	-6.0					-126.4	-151.1	-123.3	50.1
hCA II S50C Fanten; RDC jointly with PCS	3KS3	18	Tb	74.0	-23.4	-31.6	6.5	15.4	6.6	-21.0	-112.7	-2.5	18.5
		11	Yb	14.1	-6.3					-125.6	-151.3	-123.6	50.1

Note: Fanten[9] depicts tensors not in UTR but in the Fanten convention.

PCS data were fitted for each construct, using all metals simultaneously, to yield a common metal position.

For RDC only fits, the metal position of the corresponding PCS fit was given.

The joint PCS/RDC fits give only one common set of tensor parameters and metal coordinates, but separate Q factors for PCS and RDC.

Comparison of ^{1}H line width of Leu-141 in hCA II S50C tagged with Lu-M7Nitro (red) or Tm-M7Nitro (blue)

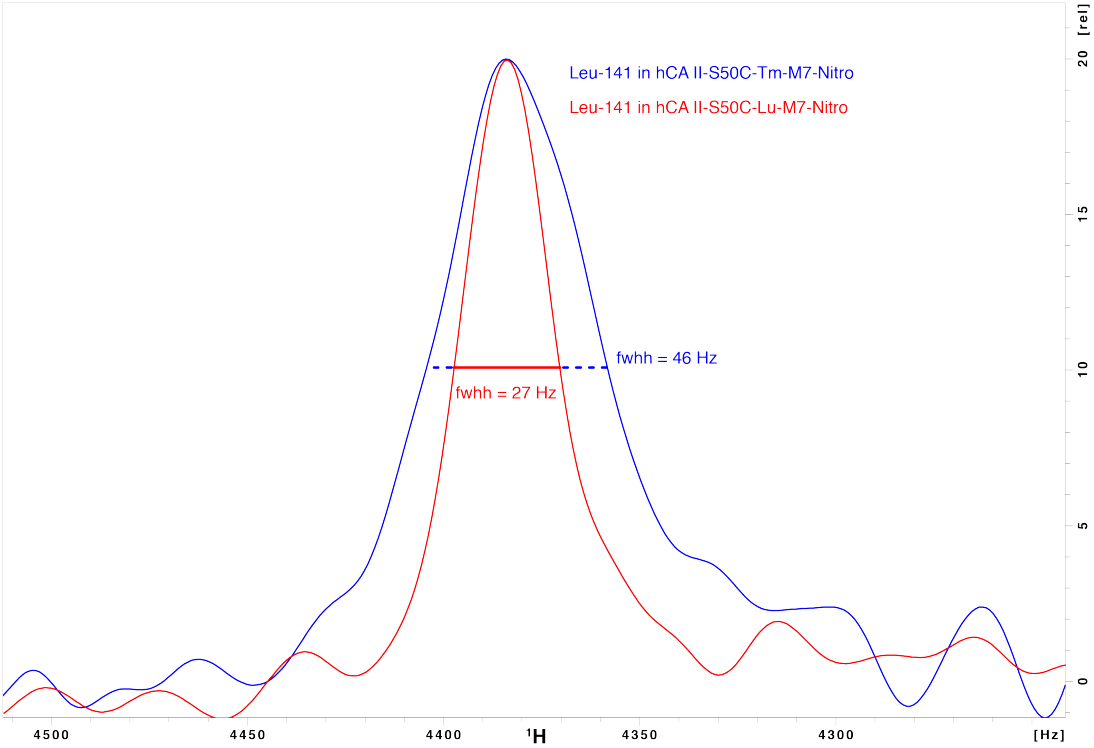

Figure S40: Comparison of the ^{1}H line width of a representative ^{1}H-^{15}N-HSQC cross peak (Leu-141) in selectively ^{15}N leucine labelled hCA II S50C tagged with Lu-M7Nitro (red) or Tm-M7Nitro (blue). The difference in line width caused predominantly by Curie line broadening amounts to ca. 20 Hz @ 600 MHz. The amide proton of Leu-141 is located 23.6 Å away from the metal position. The chemical shift offset and the intensity of the Lu-tagged spectrum were adjusted to enable direct comparison.

Comparison of tagging kinetics of Ln-M7Nitro, Ln-M7PyThiazole and M7-FPy

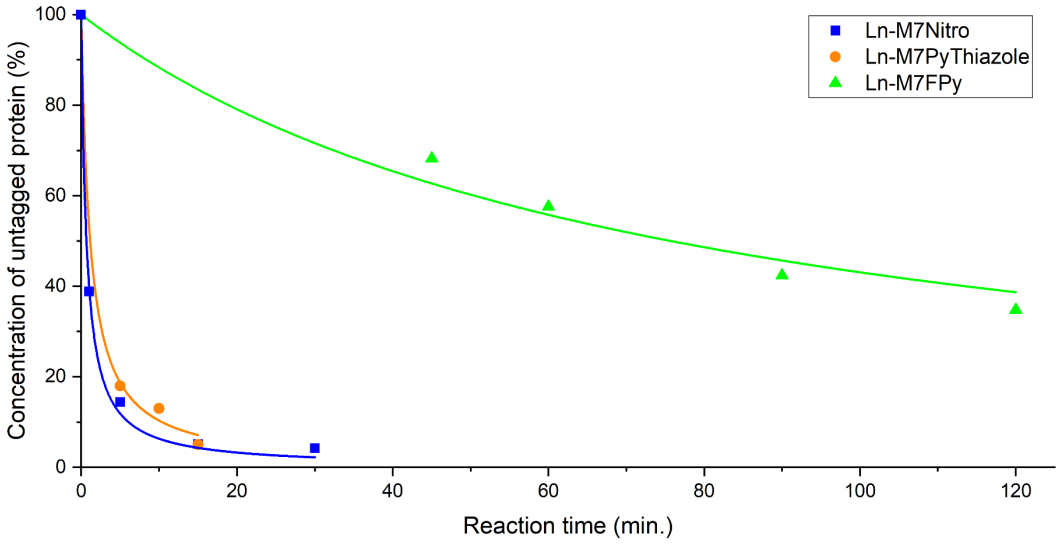

Figure S41: Comparison of tagging kinetics of Ln-M7Nitro, Ln-M7PyThiazole and Ln-M7-FPy with ubiquitin S57C. Ln-M7Nitro shows the fastest conversion of monomeric ubiquitin and tagging is complete after 30 min at rt in 10 mM phosphate buffer with pH 7.0.

References

1. Battiste, J. L.; Wagner, G. *Biochemistry* **2000**, *39*, 5355-5365.

2. Müntener, T.; Kottelat, J.; Huber, A.; Häussinger, D. *Bioconjugate Chem.* **2018**, *29*, 3344-3351.

3. Sass, J.; Cordier, F.; Hoffmann, A.; Rogowski, M.; Cousin, A.; Omichinski, J. G.; Löwen, H.; Grzesiek, S. *J. Am. Chem. Soc.* **1999**, *121*, 2047-2055.

4. Varghese, S.; Halling, P. J.; Häussinger, D.; Wimperis, S. *J. Phys. Chem. C* **2016**, *120*, 28717-28726.

5. Vranken, W. F.; Boucher, W.; Stevens, T. J.; Fogh, R. H.; Pajon, A.; Llinas, M.; Ulrich, E. L.; Markley, J. L.; Ionides, J.; Laue, E. D. *Proteins: Struct., Funct., Bioinf.* **2005**, *59*, 687-696.

6. Ramage, R.; Green, J.; Muir, T. W.; Ogunjobi, O. M.; Love, S.; Shaw, K. *Biochem. J* **1994**, *299 (Pt 1)*, 151-8.

7. Avvaru, B. S.; Kim, C. U.; Sippel, K. H.; Gruner, S. M.; Agbandje-McKenna, M.; Silverman, D. N.; McKenna, R. *Biochemistry* **2010**, *49*, 249-51.

8. Schmitz, C.; Stanton-Cook, M. J.; Su, X.-C.; Otting, G.; Huber, T. *J. Biomol. NMR* **2008**, *41*, 179.

9. Rinaldelli, M.; Carlon, A.; Ravera, E.; Parigi, G.; Luchinat, C. *J. Biomol. NMR* **2015**, *61*, 21-34.

10. Orton, H. W.; Huber, T.; Otting, G. *Magn. Reson.* **2020**, *1*, 1-12.

11. Keizers, P. H.; Saragliadis, A.; Hiruma, Y.; Overhand, M.; Ubbink, M. *J. Am. Chem. Soc.* **2008**, *130*, 14802-14812.